NANO · MICRO small
www.small-journal.com

Materials Strategies and Device Architectures of Emerging Power Supply Devices for Implantable Bioelectronics

Xueying Huang, Liu Wang, Huachun Wang, Bozhen Zhang, Xibo Wang, Rowena Y. Z. Stening, Xing Sheng, and Lan Yin**

Implantable bioelectronics represent an emerging technology that can be integrated into the human body for diagnostic and therapeutic functions. Power supply devices are an essential component of bioelectronics to ensure their robust performance. However, conventional power sources are usually bulky, rigid, and potentially contain hazardous constituent materials. The fact that biological organisms are soft, curvilinear, and have limited accommodation space poses new challenges for power supply systems to minimize the interface mismatch and still offer sufficient power to meet clinical-grade applications. Here, recent advances in state-of-the-art nonconventional power options for implantable electronics, specifically, miniaturized, flexible, or biodegradable power systems are reviewed. Material strategies and architectural design of a broad array of power devices are discussed, including energy storage systems (batteries and supercapacitors), power devices which harvest sources from the human body (biofuel cells, devices utilizing biopotentials, piezoelectric harvesters, triboelectric devices, and thermoelectric devices), and energy transfer devices which utilize sources in the surrounding environment (ultrasonic energy harvesters, inductive coupling/radiofrequency energy harvesters, and photovoltaic devices). Finally, future challenges and perspectives are given.

1. Introduction

Implantable bioelectronics are an emerging technology, which can be integrated into the human body for diagnostic and therapeutic functions—both critical for biomedicine.[1,2] Recent development of advanced materials, fabrication schemes, and device layouts have resulted in a unique set of bioelectronics. These devices are capable of intimate contact with soft, curvilinear tissues that also possess transient characteristics, paving the way for key potential improvements to human healthcare. Further, these devices facilitate continued biomedical research, for instance, soft miniaturized optoelectronic systems for wireless optogenetics, and bioresorbable electronic stents integrated with therapeutic nanoparticles to treat endovascular diseases.[3–8] Despite the great progress in implantable bioelectronics with miniaturized, flexible and bioresorbable features toward clinical standards, autonomous devices with desirable power solutions remain one of the biggest challenges to achieve remote sensing, communication and treatments in a continuous mode. Conventional power sources are usually bulky, rigid, and designed for long-term usage, and may contain potential hazardous components that require careful packaging. Representative examples include battery systems for commercially available pacemakers and deep brain stimulators.[9,10] The fact that biological organisms are soft, curved, and have limited accommodation space poses new challenges for power supply systems to minimize the interface mismatch and yet offer sufficient power to meet clinical-grade applications. Ideally, an implantable power device meets the following characteristics: miniaturized, with mechanical properties close to that of biological soft tissues, consisting of biocompatible materials with excellent device/tissue affinity, and capable of full biodegradation when designed for short or mid-term usage, eliminating the need for device retrieval. Recent innovative strategies of materials chemistry and engineering have enabled reformulating conventional power technologies into biocompatible systems in terms of constituent materials as well as mechanics formats. The development of biomaterials that blur the interface between device and tissues can further improve their

X. Huang, Dr. L. Wang, B. Zhang, X. Wang, Prof. L. Yin
School of Materials Science and Engineering
The Key Laboratory of Advanced Materials of Ministry of Education
State Key Laboratory of New Ceramics and Fine Processing
Center for Flexible Electronics Technology
Tsinghua University
Beijing 100084, P. R. China
E-mail: liuwang@mail.tsinghua.edu.cn; lanyin@tsinghua.edu.cn
H. Wang, Prof. X. Sheng
Department of Electronic Engineering
Beijing National Research Center for Information Science and Technology and Beijing Innovation Center for Future Chips
Tsinghua University
Beijing 100084, P. R. China
R. Y. Z. Stening
Department of Materials Science
Trinity College
University of Oxford
Oxford OX13BH, UK
The ORCID identification number(s) for the author(s) of this article can be found under https://doi.org/10.1002/smll.201902827.

DOI: 10.1002/smll.201902827

biocompatibility, e.g., in order to obtain excellent adhesion to tissues, mussel-inspired polydopamine (PDA)-based hydrogels were designed with superior self-healing ability, anti-freezing and anti-heating performance, high transparency, and excellent tissue affinity and adhesiveness.[11–14] Meanwhile, continuous advances in microfabrication techniques and circuit design allow the minimization of power needed for implantable bioelectronics, while still maintaining sophisticated functions. The typical power consumptions and voltage inputs of representative implantable bioelectronics are summarized in **Table 1**. As it is shown, biosensing systems typically consume less energy (<≈50 μW), where the dominant consumption likely comes from communication, analogue to digital conversion or signal amplifications and processing.[2,15,16] Radiofrequency (RF) data transmission requires ≈10 μW to 1.5 mW.[17,18] By contrast, the power needed for stimulations span a wide range, for example, 5–35 μW for pacemakers,[19] 4.5–21 mW for muscle stimulation,[20] while up to 40 mW for optical stimulation.[21,22] Further research in materials chemistry and device design that integrate various energy strategies could potentially achieve novel miniaturized biocompatible power systems that can fulfill the operational characteristics for a broader range of practical implantable electronics.

In this review, we focus on the recent advances of the state-of-art nonconventional power options for implantable electronics, specifically, miniaturized, flexible, or biodegradable power systems. First, the general design strategies of nonconventional miniaturized biocompatible power systems will be discussed. Following, a broad collection of various types of power devices, including: energy storage systems (batteries and supercapacitors); power harvesting devices that use sources from the human body (biofuel cells, devices utilize biopotentials, piezoelectric harvesters, triboelectric devices, and thermoelectric devices); or energy transfer devices, which utilize sources from the surrounding environment (ultrasonic energy harvesters, inductive coupling/RF energy harvesters and photovoltaic devices), are summarized in **Figure 1**. The materials options, integration schemes and associated performance of each category will be reviewed. Challenges and opportunities will be discussed, and perspectives on future research will be given at the end.

Xueying Huang is currently a Ph.D. student at the School of Material Science and Engineering at Tsinghua University. She received her bachelor's degree from Tsinghua University. Her research interests include biodegradable batteries and flexible electronics for implantable biomedical applications.

Liu Wang is currently doing postdoctoral research in the School of Materials Science and Engineering at Tsinghua University. She received her Ph.D. degree in the School of Materials Science and Engineering from Beijing Institute of Technology. Her current research is focusing on biodegradable materials and electronics with applications in healthcare.

Lan Yin is currently working as an Associate professor in the School of Materials Science and Engineering at Tsinghua University, China. She received her bachelor's and Ph.D. degrees from Tsinghua University and Carnegie Mellon University, respectively. Her current research is focused on biodegradable materials and electronics targeting applications for the environment and healthcare.

2. Materials and Structural Strategies of Power Devices

In general, approaches to reformulate conventional power devices into novel miniaturized biocompatible systems include both materials and architectural design. The first strategy involves introducing novel materials that are intrinsically biocompatible, flexible or biodegradable. For example, soft biopolymers and hydrogels are excellent candidates which readily adapt to soft tissues, reduce irritation and/or the foreign body response.[30,31] Inorganic materials like biodegradable metal foils (magnesium (Mg), zinc (Zn), etc.) also possess good biocompatibility, as well as high energy densities, and are therefore widely applicable as electrodes in batteries or interconnect materials in power devices.[32,33] Composite materials involving formation of networks of active materials in a biocompatible soft polymer matrix represent an alternative approach.[34] If the implantable systems are designed for short or mid-term application, biodegradable characteristics are desirable, so as to eliminate the need for a second surgery for device retrieval.[35–38] Adopting biodegradable materials into the device systems will be critically important, including the metals and oxides acting as electrodes or interconnects (Mg, Mg alloy, Zn, iron (Fe), molybdenum (Mo), silicon dioxide (SiO_2), magnesium oxide (MgO), molybdenum trioxide (MoO_3), etc.);[33,34,39,40] polymers acting as dielectrics, electrolytes or encapsulations (poly lactic-*co*-glycolic acid (PLGA), polycaprolactone (PCL), polyanhydride, alginate, etc.);[34,41] and semiconductors (silicon (Si), silicon germanium alloy (SiGe), indium–gallium–zinc-oxide (IGZO), etc.) which act as key components for diodes or transistors.[35,42–44]

Table 1. Voltage requirements and power consumptions of various categories of bioelectronics.

Categories of bioelectronics		Voltage	Power consumption	Refs.
Biosensors	Analogue-to-digital conversion	1.2–1.5 V	<35 μW	[15,16]
	Timers for biosensors	0.3–1.3 V	<660 pw	[23,24]
Communication	Radiofrequency transmitters	0.5–1.2 V	10 μW to 1.5 mW	[17,18]
	Ultrasonic transmitters	0.5–2.0 V	0.5–1.5 mW	[25,26]
Stimulation	Optical stimulation	3–3.4 V	1–40 mW	[21,22]
	Electrical stimulation	1.6–3 V	5 μW to 25 mW	[19,27,28]
	Actuators	4–4.5 V	50–100 mW	[29]

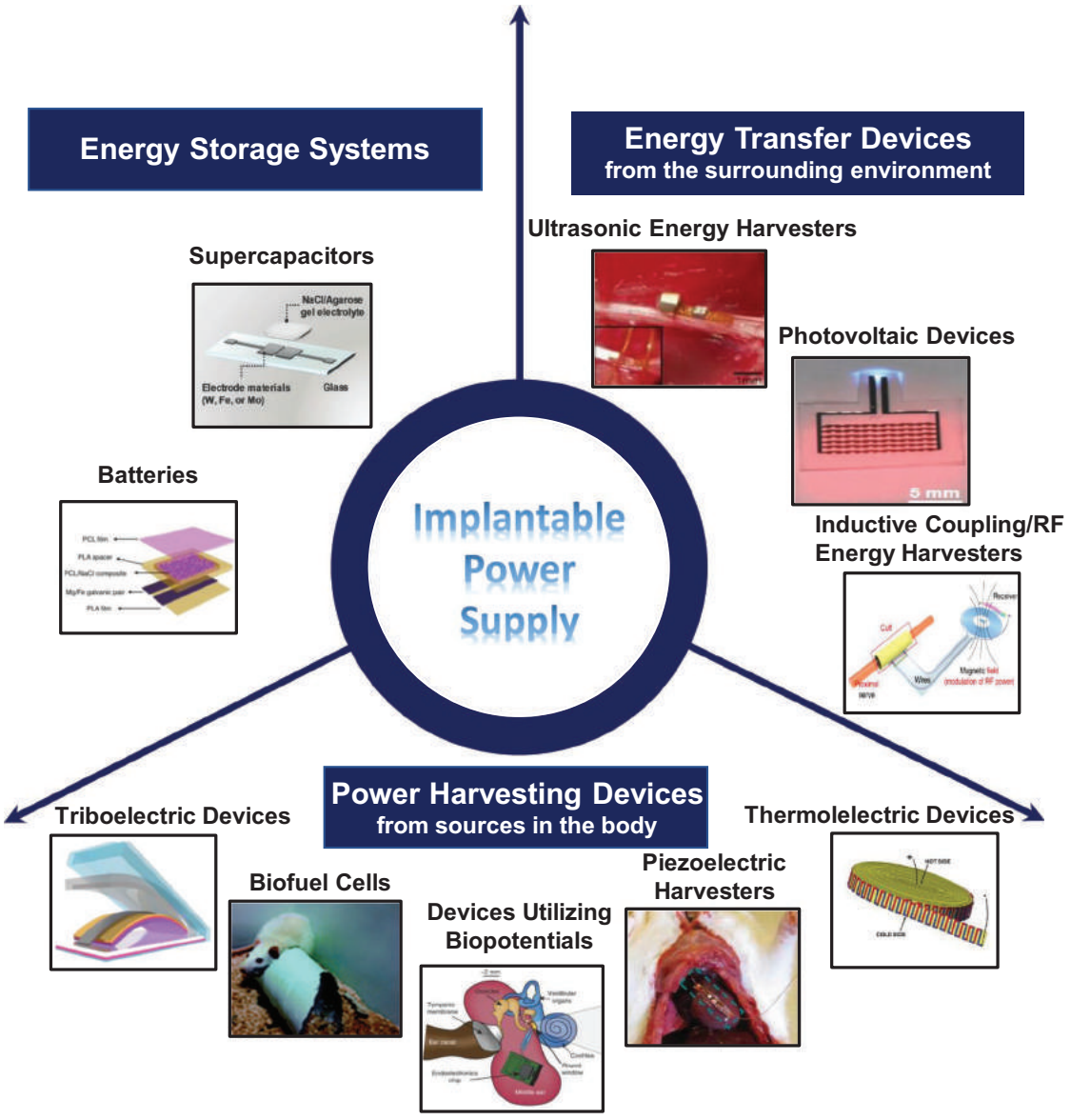

Figure 1. A collection of various types of power devices. Reproduced with permission.[41] Copyright 2019, Springer Nature. Reproduced with permission.[66] Copyright 2017, Wiley-VCH. Reproduced with permission.[91] Copyright 2008, RSC Publishing. Reproduced with permission.[106] Copyright 2012, Springer Nature. Reproduced with permission.[45] Copyright 2010, Wiley-VCH. Reproduced with permission.[139] Copyright 2016, American Chemical Society. Reproduced with permission.[147] Copyright 2006, Elsevier. Reproduced with permission.[169] Copyright 2016, Elsevier. Reproduced with permission.[32] Copyright 2018, Springer Nature. Reproduced with permission.[195] Copyright 2018, Wiley-VCH.

The second strategy incorporates mechanics and geometrical design to achieve device architectures with flexible and compact features. For example, the use of rigid inorganic materials in nanowire or thin film format enables accommodate of relatively large deformations but does not induce significant strain in the materials.[6,45] Introducing serpentine or buckling structure of semiconductors or interconnects can further enhance the capability to adapt deformation without sacrificing electrical performance.[46] In addition, in order to further maintain electrical stability, island-bridge configurations which leave the semiconductor components in their flat format, but transform the metal interconnects into stretchable wavy forms can be utilized.[8] 3D coiling or stacking structures formed through novel fabrication techniques allow miniaturization of power devices.[47,48] Nevertheless, depending on the type of power devices, size reduction could still sacrifice power capacity. Biocompatible high energy materials, novel structure schemes as well as ultralow power electronics design are potential solutions. Various emerging nonconventional power supply systems will be discussed in details in the following sessions.

3. Energy Storage Systems

3.1. Batteries

Batteries play an indispensable role in powering implantable bioelectronics, as they have high energy density, excellent cyclic stability, and can be deployed in most physiological environments. Since the 1960s, lithium batteries have been used as power sources for pacemakers and other implantable medical devices (IMDs).[49] Despite their wide usage, conventional implantable battery systems are bulky, rigid, and possess the risk of hazardous material leakage. Exploring new materials chemistry and reformulating battery structure is therefore necessary to ensure novel miniaturized biocompatible battery systems that can match the soft nature of the human body. In these emerging systems, achieving sufficient capacity is essential in order to satisfy the power consumption of the targeting implantable electronics and avoid the need for charging through external energy transfer devices, which might not be practical in deeper regions of the body.[2]

Biocompatible metallic electrodes (e.g., Mg and Zn) with high energy density in the thin-film or thin-foil format, acting as the anodes represent one widely adopted strategy to achieve both biocompatible and flexible battery implants.[50,51] Coupled with biocompatible thin-film cathode materials (e.g., platinum (Pt), copper (Cu), gold (Au), polypyrrole (PPy)), the constructed galvanic cells can offer electrical power through the electrochemical dissolution process of the active materials (Mg, Zn). Biofluids or biopolymer materials serves as the electrolyte, which circumvents the usage of hazardous solvents as that in general lithium-ion battery.[51,52] A miniaturized and flexible Mg–Cu and Zn–Cu galvanic cell, reported by Nadeau et al., is shown in **Figure 2**a.[51] The prolonged energy collection system can provide a voltage of 0.2 V and power density of 2.3 $\mu W\ mm^{-2}$ by 1 mm^2 Zn–Cu cell, enabling in vivo temperature sensing and wireless communication in the gastrointestinal tract in a pig model. The device also uses the harvested energy to activate drug release through the electrochemical dissolution of the Au film. The work from Proteus Digital Health proposed a highly integrated platform for measuring medication ingestion and adherence in real-time, which employed a Mg–CuCl battery that utilizes gastric fluid as the electrolytic solution.[53] Mg alloy and biocompatible polypyrrole-*para*(toluene sulfonic acid) (PPy-pTS) films have been reported as the anode and cathode materials respectively, as shown in Figure 2b, and a maximum volumetric power density of 3.9 $W\ L^{-1}$ is achieved.[52] Flexible silk fibroin thin films have also been reported as an alternative cathode material for a Mg–air battery, and they are disintegrable in the concentrated buffered protease XIV solution (lost 82% mass after 15 days).[54] Moreover, room temperature liquid metals can also potentially serve as the electrode components in building flexible implantable battery.[55,56]

For temporary biomedical implants, fully biodegradable battery system eliminating unnecessary materials retention in the human body after usage is attracting significant attention. Batteries with all dissolvable materials have been proposed to build fully degradable systems. Materials candidates include biodegradable metals (Mg, Zn, Fe, tungsten (W), Mo et al.),[33] dissolvable oxides (MoO_3),[34] and biodegradable polymers or hydrogels (e.g., PLGA, alginate)[34,41] as the electrolyte and encapsulation materials. A fully biodegradable Mg–MoO_3 battery reported by Huang et al. appears in Figure 2c.[34] A stable voltage up to 1.6 V and the power density of 0.27 $mW\ cm^{-2}$ is achieved. The battery is shown to be fully degradable both in vitro and in vivo, and the cell toxicity and biocompatibility evaluation in rats do not show any significant adverse effects. Tsang et al. reported continuous progress on miniaturized biodegradable Mg–Fe galvanic cells, and a representative structure appears in Figure 2d.[57] An energy density of 694 $Wh\ kg^{-1}$ with a 0.02 cm^3 total volume is achieved.[57,58] As shown in Figure 2e, the introduction of dry electrolyte (PCL films) with preloaded salts enables water activated Mg–Fe batteries with prolonged storage time and allows performance relatively independent of the external biofluids environment.[41]

Miniaturized metal ion batteries powered with aqueous solutions offer another biocompatible power solution for implantable batteries and can enable rechargeability. Sodium, potassium, and magnesium ion batteries are of particular interest, as these ions are already present in the human body. The choice of electrode materials suitable for the reversible storage/release of ions over a sufficient lifetime remains a challenge. Kim and Bettinger have reported miniaturized, edible sodium-ion batteries made using activated carbon (AC) and manganese dioxides (MnO_2) as the anode and cathode respectively, as shown Figure 2f.[59] The battery is packaged in gelatin capsules and can be deployed upon activation in the stomach, and a voltage of 0.6 V and current of 20 μA can be generated. Kim et al. further developed an edible sodium-ion battery with an output voltage of up to 1.03 V based on bioderived melanin and MnO_2 electrodes.[60] A schematic graph of another melanin-based sodium ion full cell is shown in Figure 2g, which was fabricated by silver nanowire (AgNW) cathodes along with sodium titanium phosphate (NTP, $NaTi_2(PO_4)_3$) anodes, and may also be used as the power supply for ingestible and implantable medical devices.[61] The melanin electrode can also be used as the electrode for Mg^{2+} rechargeable batteries through catechol-mediated

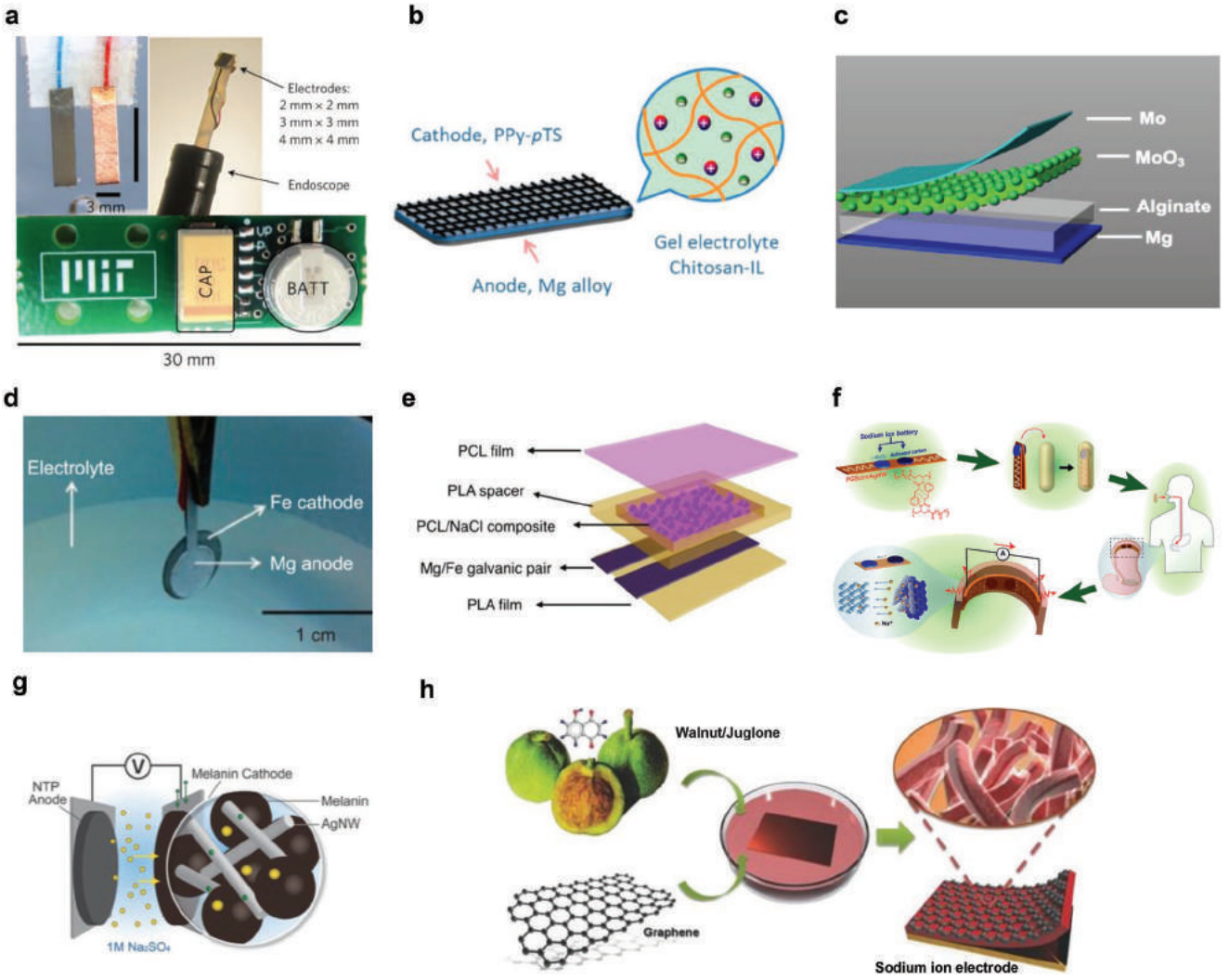

Figure 2. Implantable batteries: a) An implantable energy system powered by a miniaturized Zn/Mg–Cu cell. Reproduced with permission.[51] Copyright 2017, Springer Nature. b) An implantable battery composed of Mg alloy and biocompatible PPy-pTS. Reproduced with permission.[52] Copyright 2014, American Chemical Society. c) A fully biodegradable Mg–MoO_3 battery. Reproduced with permission.[34] Copyright 2018, Wiley-VCH. d) A miniaturized biodegradable Mg–Fe galvanic cell. Reproduced with permission.[57] Copyright 2015, Springer Nature. e) A water-activated Mg–Fe battery with preloaded dry electrolyte. Reproduced with permission.[41] Copyright 2019, Springer Nature. f) A miniaturized edible sodium ion batteries. Reproduced with permission.[59] Copyright 2013, Royal Society of Chemistry. g) A schematic of sodium ion full battery based on melanin and NTP electrodes. Reproduced with permission.[61] Copyright 2016, Wiley-VCH. h) A sodium ion battery based on the redox reactions of quinone groups. Reproduced with permission.[65] Copyright 2015, Wiley-VCH.

reversible binding of multivalent cations (Mg^{2+}). A reasonable charge storage capacity (61.6 mAh g^{-1}) and cycling stability (over 500 cycles) in melanin half-cells has been realized.[62] Besides melanin, biomaterials like polydopamine (PDA),[63,64] juglone[65] are all proposed as electrodes for metal ion batteries. As shown in Figure 2h, combined with the redox activity of quinone groups in Juglone and the high conductivity of redox graphene oxides nanosheets, a sodium-ion battery with high storage capacity and cycling stability is achieved.[65] Future exploration of the use of these biomaterials in implantable battery systems is an area of potential interest.

Overall, batteries represent the essential approach in supplying power for IMDs. Further optimization of materials chemistry and battery architecture will enable biocompatible, flexible and biodegradable battery systems with more desirable performance. Biocompatible organic materials provide alternative electrode choices. Moreover, strategies to trigger and interact with implantable batteries upon and after deployment will offer more versatile functionalities.

3.2. Supercapacitors

Supercapacitors offer an important alternative energy option for implantable bioelectronics, as they have superior power densities, charge/discharge rates, and cycle lifetime compared to batteries. In contrast to batteries, supercapacitors store energy either through ion adsorption or redox reactions at the interface

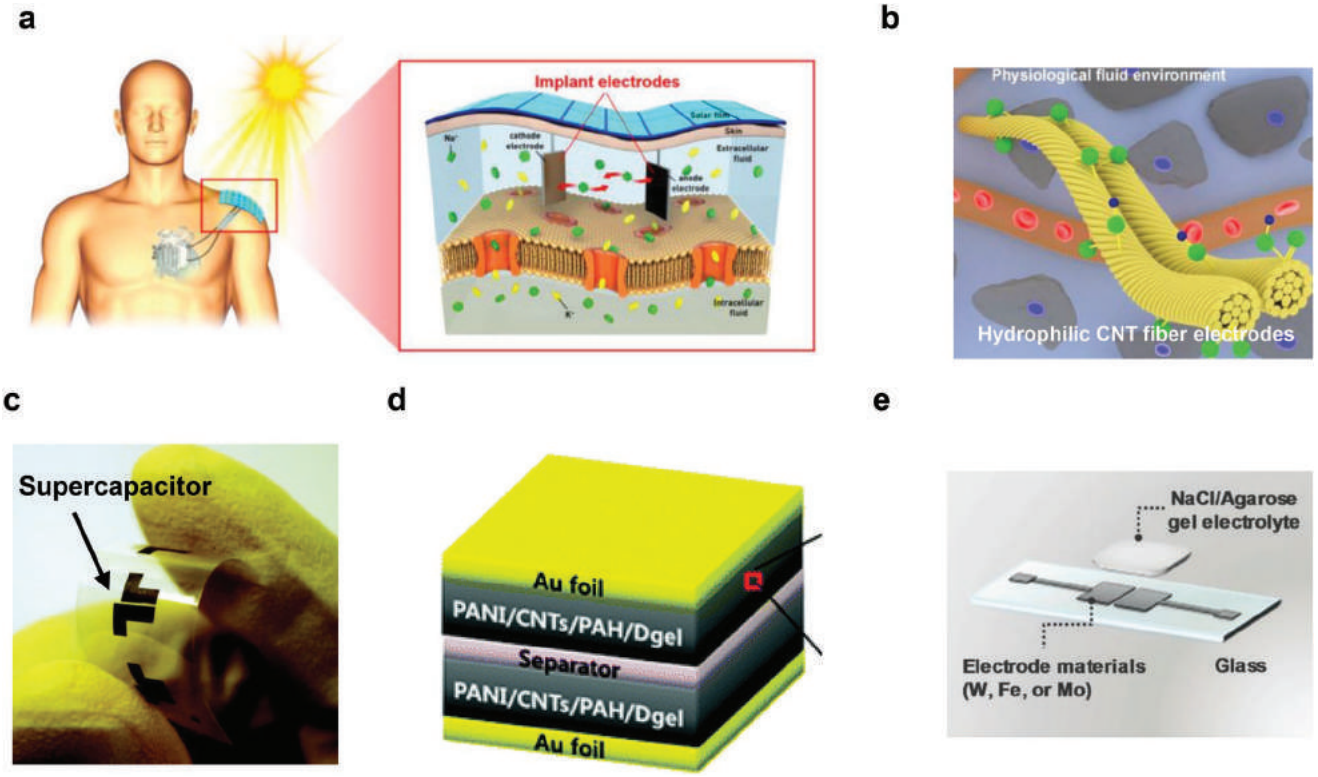

Figure 3. Implantable supercapacitors: a) A supercapacitor consisting of MnO_2 and carbon materials implanted into the subcutaneous layer of the rat's skin. Reproduced with permission.[75] Copyright 2017, Elsevier. b) A biocompatible supercapacitor consisting of hydrophilic CNT fibers. Reproduced with permission.[69] Copyright 2017, Elsevier. c) A melanin-based supercapacitor. Reproduced with permission.[73] Copyright 2013, Royal Society of Chemistry. d) A high performance supercapacitor with porous DNA hydrogel as the template. Reproduced with permission.[76] Copyright 2013, Royal Society of Chemistry. e) A fully biodegradable and edible supercapacitor. Reproduced with permission.[66] Copyright 2017, Wiley-VCH.

between the electrode and electrolyte. Although their power densities are generally lower compared to those of battery systems, supercapacitors can be integrated with other energy harvesting systems and provide rapid energy storage. By incorporating various materials in the thin film formats, including metals, oxides,[39,66,67] silicon,[68] carbon materials,[69–72] and organic polymers,[73] supercapacitors can be reformulated into novel, flexible, stretchable, and biodegradable (or edible) systems that can better adapt to the human body.[70–72,74] Chae et al. implanted two biocompatible hybrid electrodes fabricated by MnO_2 and carbon into the subcutaneous layer of rat's skin as shown in **Figure 3**a, demonstrating a stable supercapacitor performance (0.2–1 V at 2 mA) for 5000 cycles.[75]

Flexibility is an essential property for implantable supercapacitors. Carbon materials have been widely used for flexible and stretchable supercapacitors.[70–72] Based on carbon material and the prestraining-then-buckling approach, a stretchable, wire-shaped supercapacitor can maintain its electrochemical properties at 0–100% tensile strains, or after 20 mechanical strain-release cycles.[72] As shown in Figure 3b, a biocompatible and flexible supercapacitor consisting of hydrophilic carbon nanotubes (CNT) fibers can work in phosphate-buffered solution (PBS), serum and blood, maintaining a capacitance of 20.8 F g^{-1} by 98.3% after 10 000 cycles.[69] Polymers including natural biomolecules also present their potential to be used in flexible supercapacitors, including melanin,[73] deoxyribonucleic acid (DNA) hydrogel,[76] ferritin.[77] Kumar et al. presented a specific capacitance of 167 F g^{-1} based on melanin materials, with a calculated maximum power density of melanin supercapacitors of up to 20 mW cm^{-2}, suggesting that melanin could be an effective candidate for future flexible supercapacitor electrodes (Figure 3c).[73] Alternatively, the porous DNA hydrogel is used as an excellent template for the combination of CNT and polyaniline (PANI) to produce high-performance supercapacitors, as illustrated in Figure 3d.[76]

Biodegradable and edible supercapacitors have also been proposed.[66,67,74] As shown in Figure 3e, Lee et al. reported the first biodegradable supercapacitors using water-soluble metallic electrodes and an agarose electrolyte. A capacitance of 1.6 mF cm^{-2} and power density of 1 mW cm^{-2} is obtained.[66]

4. Power Harvesting Devices Utilize Sources from the Human Body

4.1. Biofuel Cells

Implantable biofuel cells based on catalytic reactions of biochemicals (e.g., glucose) are alternative power sources for IMDs, with the advantage of sustainable power supply provided fuels are available. The most widely used biofuel is glucose, as it is readily available in the human body. The redox reactions of biofuels

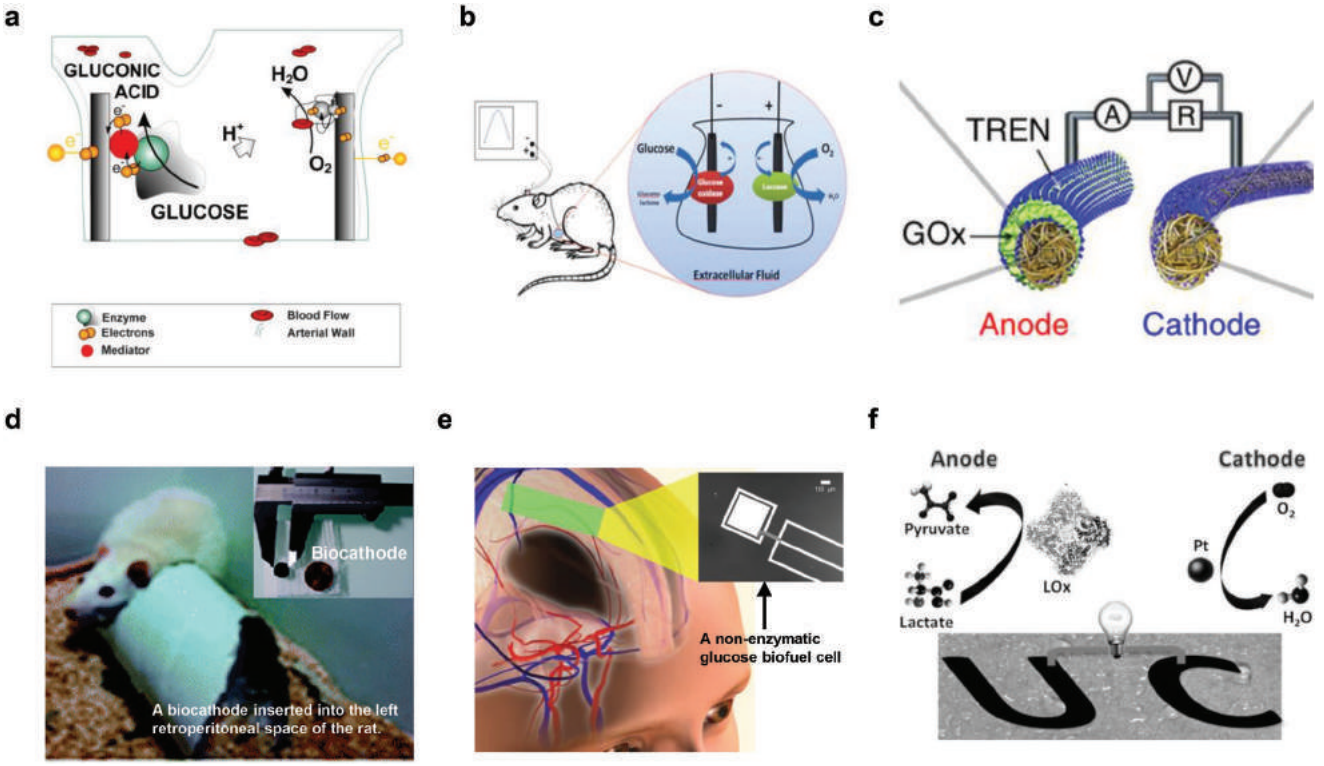

Figure 4. Biofuel cells: a) The scheme of working principle of implantable glucose biofuel cells in the blood vessel. Reproduced with permission.[82] Copyright 2010, MPDI AG. b) A glucose biofuel cell based on glucose oxidase and laccase on CNT implanted in the abdominal cavity of a rat. Reproduced with permission.[92] Copyright 2013, Springer Nature. c) A layer-by-layer (LBL) assembly GOx-coated metallic cotton fibers for glucose biofuel cells. Reproduced with permission.[93] Copyright 2018, Springer Nature. d) A chitosan (Chit)-MWCNT cathode crosslinked by genipin enclosed within a Dacron bag and inserted into the retroperitoneal space of rat. Reproduced with permission.[91] Copyright 2008, RSC Publishing. e) Conceptual schematic design of nonenzymatic glucose biofuel cell implantation composed of activated nanostructured Pt anode and SWCNT cathode. Reproduced with permission.[99] Copyright 2012, Public Library of Science. f) A noninvasive epidermal biofuel cell. Reproduced with permission.[100] Copyright 2013, Wiley-VCH.

are devoted to the power source, with three main approaches to harvest chemical energy, i.e., microbial, enzymatic, and nonenzymatic types. Microbial oxidation at the anode is the most effective method, however, the large device carrying microorganisms is not suitable for implantation.[78] In contrast, after the first demonstration by Yahiro et al.,[79] it is suggested that enzymatic glucose biofuel cells (GBFC), based on glucose oxidase could be implanted in blood vessels to extract electricity.[80,81] The representative structure is shown in **Figure 4**a.[82] The catalytic oxidation of glucose at the anode and the reduction of oxygen at the cathode in the blood vessels converts electrochemical energy into electrical energy. Although the deployment in blood vessel has not been realized yet due to various fundamental and technological issues, the enzymatic biofuel cells have been successfully implanted in biological organs and tissues of many creatures, including plants (grape[83] and cactus[84]), invertebrates (cockroaches,[85,86] snail,[87] clam,[88] and lobster[89]) and vertebrates (rats[90–92] and rabbits[83]). Figure 4b shows a glucose biofuel cell based on glucose oxidase and laccase on CNT implanted in the abdominal cavity of a rat, proving glucose in the body could serve as the only energy source, producing an open circuit voltage of 0.57 V and power density of 193.5 μW cm^{-2}.[92] The introduction of nanomaterials (i.e., multiwalled carbon nanotubes (MWCNT),[88] gold nanoparticles (AuNP),[93] and platinum nanoparticles (PtNP)[94]) effectively decreases the device volume and improves the power density of glucose biofuel cells (up to 3700 μW cm^{-2}), as shown in Figure 4c. The use of Buckypaper,[87–89] carbon films,[94] and polymers[95] in glucose biofuel cell also increases the mechanical flexibility of the cells. Due to biofouling, enzyme degradation, and the inflammatory response, general glucose fuel cells have a very limited lifetime (from several hours to days),[96] which may not match the requirements of IMDs designed for longer-term usage. The introduction of a chitosan (Chit)-MWCNT cathode, crosslinked by genipin which can enhance the matrix and enzyme immobilization, as well as prevent the degradation of the chitosan, improve the lifetime of the cell by up to 167 days, demonstrating the potential for long-term energy supply, as shown in Figure 4d.[91]

On the other hand, the nonenzymatic biofuel cells have the advantages of easy assembly and eliminate the enzyme degradation issues, although the power efficiencies are lower (<40 μW cm^{-2}) compared to the enzymatic fuel cells (193.5 μW cm^{-2}).[97,98] Nevertheless, the advances in semiconductor fabrication techniques promote the performance of nonenzymatic biofuel cells. As illustrated in Figure 4e, a nonenzymatic biofuel cell, fabricated by a complementary metal–oxide–semiconductor (CMOS) process, composed of activated nanostructured Pt anodes and single-walled carbon nanotubes (SWCNT) cathodes, achieves a steady-state power of 3.4 μW cm^{-2} and a peak power up to 180 μW cm^{-2}.[99] By using the cells, it is

expected that at least 1 mW could be harvested from the natural recirculation of the cerebrospinal fluids around the human brain.

In addition, the diversity of biofuels has been constantly expanded given the abundant biochemicals in the living body. Lactate[100–102] has been shown to be useful in various medical devices, and as shown in Figure 4f, the power density, ranging from 5 to 70 μW cm^{-2}, is generated by noninvasive epidermal biofuel cells, through the oxidation of lactate in perspiration (at the lactate oxidase functionalized anode) and reduction of oxygen at the Pt-black-modified carbon cathode. By using mitochondria as the catalyst, pyruvate acid,[103] succinate acid,[104] fatty acids,[103] and amino acids[105] have also been shown to have potential applications in biofuel cells at the subcellular level.

4.2. Devices Utilize Biopotentials

Taking advantages of biopotential existing in the human body could be another power source for implantable devices. Endocochlear potential (EP) produced by potassium ion transfer between the perilymph and the endolymph offers the largest positive direct current electrochemical potential (70–100 mV) in mammals.[106] As given in **Figure 5**a, an ultralow power wireless signal device can be supported for up to 5 h by the endocochlear potential of a guinea pig, using two miniaturized glass beveled microelectrodes (1 μm in diameter) inserted into the endolymph and perilymph. On the other hand, the membrane potential, caused by the transfer of ions (such as potassium (K) and sodium (Na) ions) across channels and pumps on the electrically polarized cell membrane, is not limited by location, and therefore, easier to harvest than the endocochlear potential. Catacuzzen has harvested electrical energy from female frog cells and enabled the operation of a wireless device, using a silver/silver chloride (Ag/AgCl) intercellular electrode and two voltage-clamps, demonstrating the possibility of utilizing membrane potential.[107] Inspired by electrical eels (Figure 5b), the accumulation of membrane potential caused by the stacks of electrically polarized biocells can be devoted to high voltage and current output, illustrating the potential applications of membrane potential in IMDs.[108]

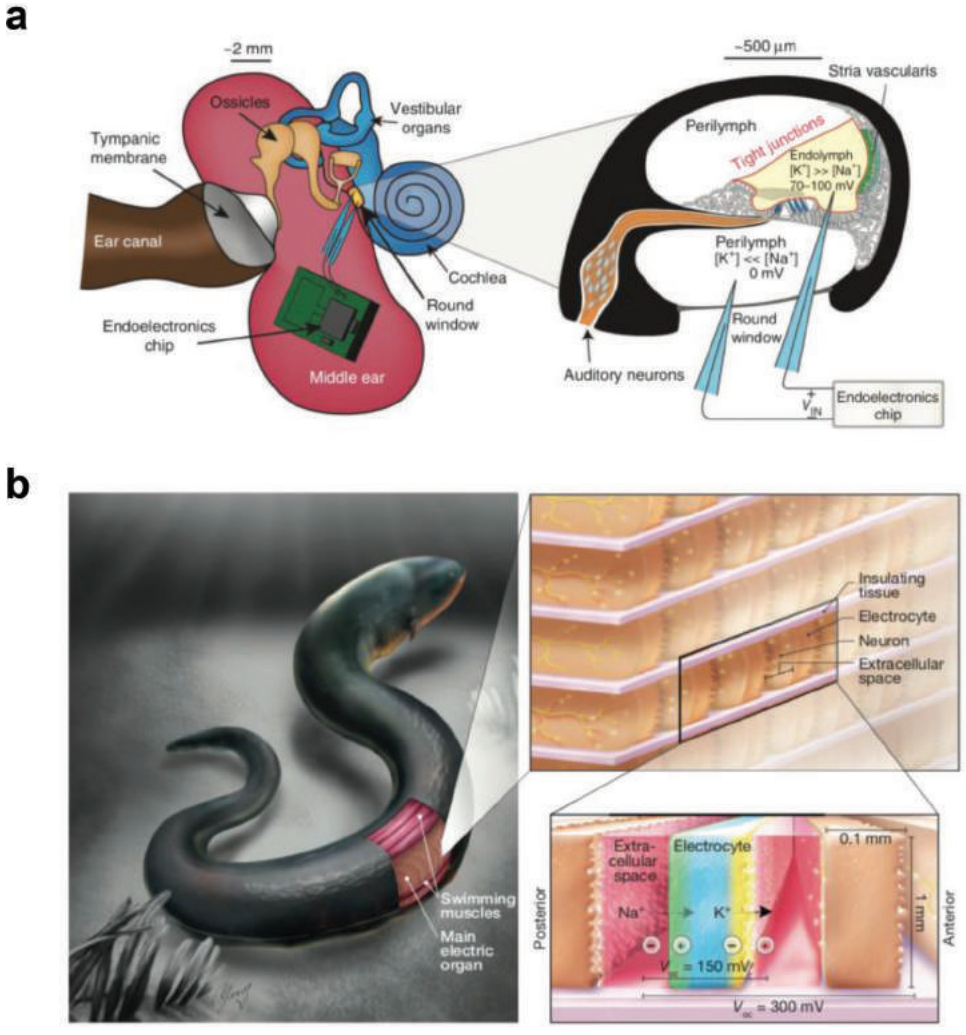

Figure 5. Devices utilizing biopotentials: a) Endocochlear potential caused by the transfer of potassium ion between perilymph and endolymph. Reproduced with permission.[106] Copyright 2012, Springer Nature. b) The accumulation of membrane potential caused by the stacking of electrical polarized biocells. Reproduced with permission.[108] Copyright 2017, Springer Nature.

In addition, biopotentials existing in many organs (heart, brain, and retina) are also worth exploring as potential power sources for IMDs.

4.3. Piezoelectric Harvesters

By converting the mechanical motions of the human body (e.g., heartbeat, breathing, etc.) directly into electrical energy, piezoelectric energy harvesters (PEHs) have been demonstrated to be a potential power supply for IMDs, with the advantages of high power density, simple architecture, and good scalability.

Lead zirconate titanate (PZT) represents the most widely used piezoelectric material,[109–112] although other more biocompatible alternatives have also been developed, including zinc oxide (ZnO),[45,113,114] barium titanate ($BaTiO_3$),[115] piezoelectric polymers (e.g., polyvinylidene fluoride (PVDF), electrospun poly(L-lactic acid) (PLLA),[116–121] and bio-piezoelectric materials (bacterial viruses (M13 phase), fish swim bladder[122,123]). Most high performance inorganic piezoelectric materials are rigid and brittle. In consideration of the soft and irregular surfaces of biological tissue, structural reformulation (nanowires, thin films, etc.), and integration with soft materials are necessary to achieve the high flexibility and sensitivity necessary to avoid causing any damage to the tissues. **Figure 6**a,b illustrates the first implanted flexible piezoelectric harvester based on single ZnO nanowires in a male SD rat producing an alternating current. The output voltage and current are around 3 mV and 30 pA, respectively.[45] In contrast to conventional cantilever structure, Deterre et al. designed a microspiral-shape piezoelectric energy harvester packaged by 10 µm deformable ultraflexible electrodeposited microbellows, creating a miniaturized high-density (6 µJ cm^{-3} per cycle) energy harvester with a size of 6 mm in diameter and 21 mm^3 in volume. Such an energy harvester could collect energy from blood pressure variations in the cardiac environment and serve as life-lasting leadless pacemakers.[124] By using intrinsically soft polymers and thin film metallic interconnects, Zhang et al. proposed a flexible piezoelectric energy nanogenerator (PENG) based on a PVDF membrane with a size of 2.5 cm × 5.6 cm × 200 µm. The device is implanted by wrapping it around the ascending aorta in a pig (Figure 6c).[116] An electrical potential of 1.5 V and 300 nA

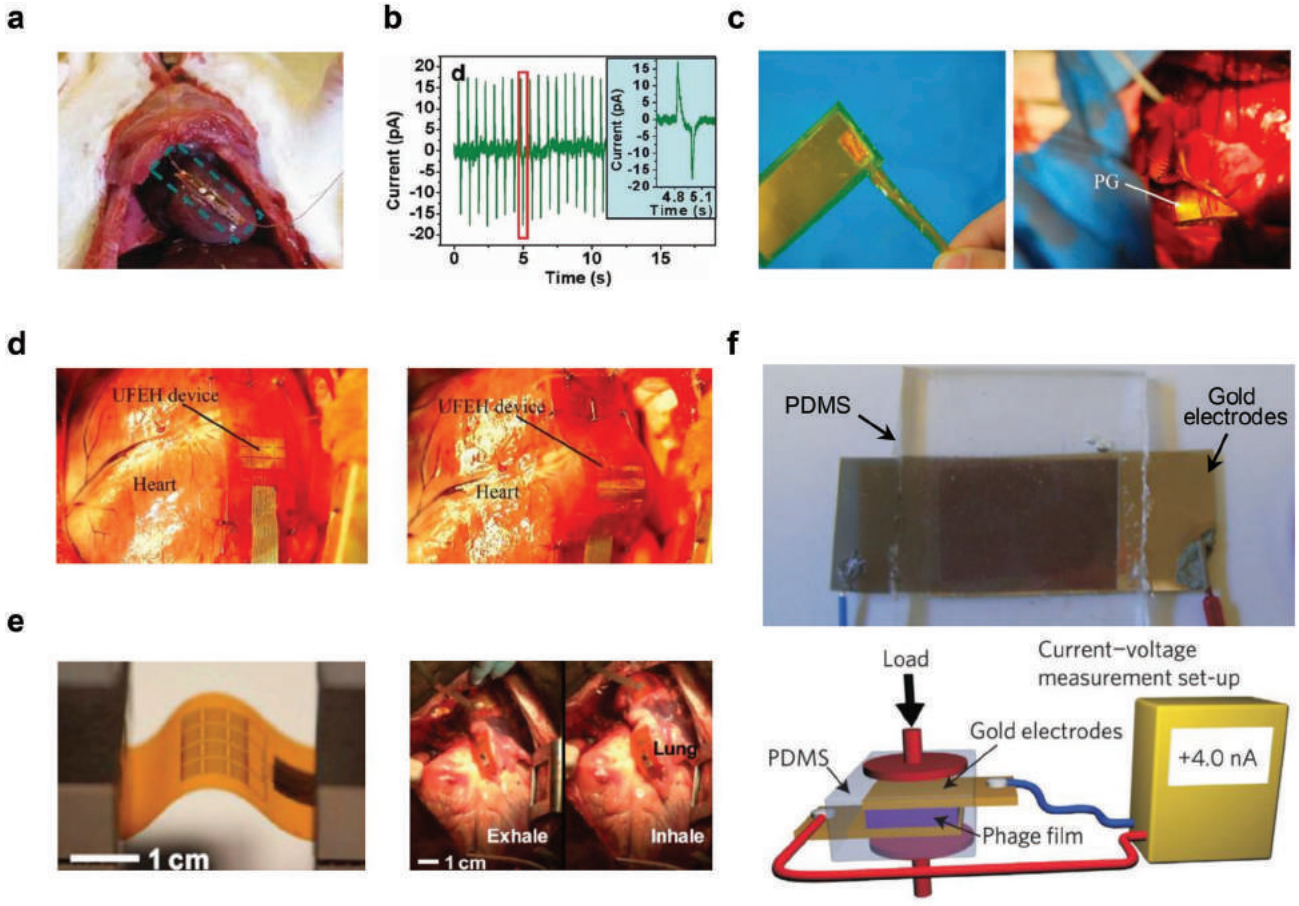

Figure 6. Implantable piezoelectric harvesters: a,b) The first implanted flexible piezoelectric harvester based on single ZnO nanowire in a male SD rat. Reproduced with permission.[45] Copyright 2010, Wiley-VCH. c) A flexible piezoelectric energy nanogenerator (PENG) implanted around the ascending aorta of a porcine. Reproduced with permission.[116] Copyright 2015, Elsevier. d) An ultraflexible energy harvester (UFEH) collecting biomechanical energy under different physiological conditions in pigs. Reproduced with permission.[111] Copyright 2015, Springer Nature. e) A flexible piezoelectric harvester based on PZT thin films. Reproduced with permission.[110] Copyright 2014, National Academy of Sciences. f) A piezoelectric energy harvester assembled by modified M13 phase. Reproduced with permission.[122] Copyright 2012, Springer Nature.

is obtained from the pulsation of the blood vessels. Figure 6d presents the implantation of ultraflexible ceramic PZT thin-film piezoelectric devices to harvest biomechanical energy under different physiological conditions in pigs, including the opening or closing of the thoracic cavity, and the status of being awake or under anesthesia.[111] The obtained peak-to-peak voltage is as high as 3 V, which is comparable to the input required by typical biomedical devices such as commercial pacemakers. Another example of a flexible piezoelectric harvester based on PZT thin-films appears in Figure 6e, and it is implanted to harvest the energy from movements of the heart, lung, and diaphragm of bovine and ovine, demonstrating that a stable (over 20 million bending/unbending cycles), complete and integrated piezoelectric energy harvesting system can be applied on large animals with organ size approaching the human scale.[110]

Further, piezoelectric harvesters built on biodegradable piezoelectric materials can physically disappear after usage and avoid a second surgery for device retrieval. Dagdeviren et al. has proposed a piezoelectrical device consisted of water soluble materials (ZnO, Mg, MgO, and silk), which completely dissolve in deionized water within 60 min at room temperature, a representative illustration of a biodegradable piezoelectric energy harvester.[113]

Moreover, biomaterials like piezoelectric microorganisms and organics with a short life time have also attracted significant attention. Lee et al.[122,125] proposed a piezoelectric energy harvester assembled by a modified M13 phase (bacterial viruses), and flexible chromium/gold (Cr/Au) thin-films, which could generate electrical potential of 6 nA and 400 mV to operate a liquid-crystal display (Figure 6f).[122] Moving forward, silk, bone, swim bladder, and other bio-piezoelectric materials are also of exploratory interest.

4.4. Triboelectric Devices

Similar to piezoelectric energy harvesters, the triboelectric nanogenerator (TENG) represents an alternative power solution to convert random mechanical energy in the body into electric power. TENG utilizes the conjunction of triboelectrification and electrostatic induction resulting from the frictional charge separation between different materials with opposite triboelectric polarities, which shows unique advantages, including simple fabrication, low-cost manufacturing, universal feasibility, and durability.[126–129] A TENG generally consists of two sheets of organic/inorganic films that exhibit distinctly different electron-attracting abilities, with one electrophilic and the other electrophobic. Alternating potential difference will be induced upon cycled separation and recontact of the opposite triboelectric charges on the surface of the materials.[130–132]

The material properties, including the electron affinity, related to the surface charge density; surface roughness, related to the triboelectrification characteristic; the work function, and so on, play important roles in the output performance of a TENG. A wide range of materials have been explored to build flexible TENG, including intrinsically flexible polymers or thin-film inorganic conductors. For example, Kapton, silk, polytetrafluoroethylene (PTFE), PVDF, fluorinated ethylene propylene (FEP), and poly(1*H*,1*H*,2*H*,2*H*-perfluorodecylmethacrylate) (PFDMA) are used for negatively charged triboelectric materials;[133–136] nylon, Al, Cu, and polymethyl methacrylate (PMMA) are used for positively charged triboelectric materials;[134,137] and Teflon, PTFE, and polydimethylsiloxane (PDMS) are used for substrates or encapsulations.[134,136–139] A typical stacked arch-shaped structure of TENG appears in **Figure 7**a.[139] Other alternative structures include a spring configuration consisting of alternatively stacked arch-shaped and anti-arch-shaped structures,[140] and the in-plane sliding structure.[135]

Various TENGs have been demonstrated as a potential flexible biomechanical energy harvester for self-powered IMDs.[134,136] Figure 7b shows an implantable pacemaker powered by a flexible TENG which harvests energy from the periodic breathing in a living rat. This TENG consists of Al-foil (contact layer and one electrode), Au film (the other electrode), a thin Kapton substrate, and PDMS films (encapsulation) creating on a fully packaged structure. The output open-circuit voltage and short-circuit current of this TENG with overall size of 1.2 × 1.2 cm is about 12 V and 0.25 μA, respectively, and the power density can reach up to 8.44 mW m^{-2}.[134] However, the generated energy is much lower than that needed by the human body, as the rats are much smaller. A flexible TENG with high output performance in large-scale animals, driven by the heartbeat of adult pigs was achieved, and the device structure is given in Figure 7a. Figure 7c shows the in vivo output performance of the TENG in an adult Yorkshire porcine. It is composed of a multilayered structure with nanostructured PTFE as the triboelectric layer, Kapton film as a flexible substrate, an Au layer as one electrode, and Al-foil as the other triboelectric layer and electrode. The in vivo output voltage and the corresponding current can reach 14 V and 5 μA, respectively, and the implanted TENG is demonstrated to continuously generate electricity for over 72 h in the active porcine.[139] Furthermore, a fully implanted symbiotic pacemaker, based on a flexible TENG, has been shown to successfully achieve energy harvesting as well as cardiac pacing and sinus arrhythmia correction on the large animal model. Figure 7d shows the in vivo energy harvesting process driven by the diastole and systole of the heart. This TENG consists of a triboelectric layer (nanostructured PTFE), a spacer (ethylene-vinyl acetate copolymer, EVA), keel (titanium), and encapsulation layers (Teflon film and PDMS) based on a core–shell structure. The open-circuit voltage and the corresponding short-circuit current of this TENG reaches up to 65.2 V and 5.9 μA, respectively. Long-term output stability of this TENG testing using an accelerate fatigue test shows that the open-circuit voltage can maintain a voltage of 95 V after 100 million mechanical stimuli cycles (completed using a vibration table), as presented in Figure 7e.[136] Moreover, a "smart" vagus nerve stimulation system, powered by a flexible TENG, which can reduce food intake and achieve weight control by yielding electric signals in responsive to the peristalsis of the stomach is demonstrated, as presented in Figure 7f.[141]

In addition to flexibility, biodegradability is another important characteristic to be considered for implantable biomedical applications. Demonstrated materials candidates for biodegradable TENGs include silk, poly(lactic) acid (PLA), gelatin, PLGA, poly(3-hydroxybutyric acid-*co*-3-hydroxyvaleric acid) (PHB/V), PCL, chitosan, and poly(vinyl alcohol) (PVA) as the triboelectric

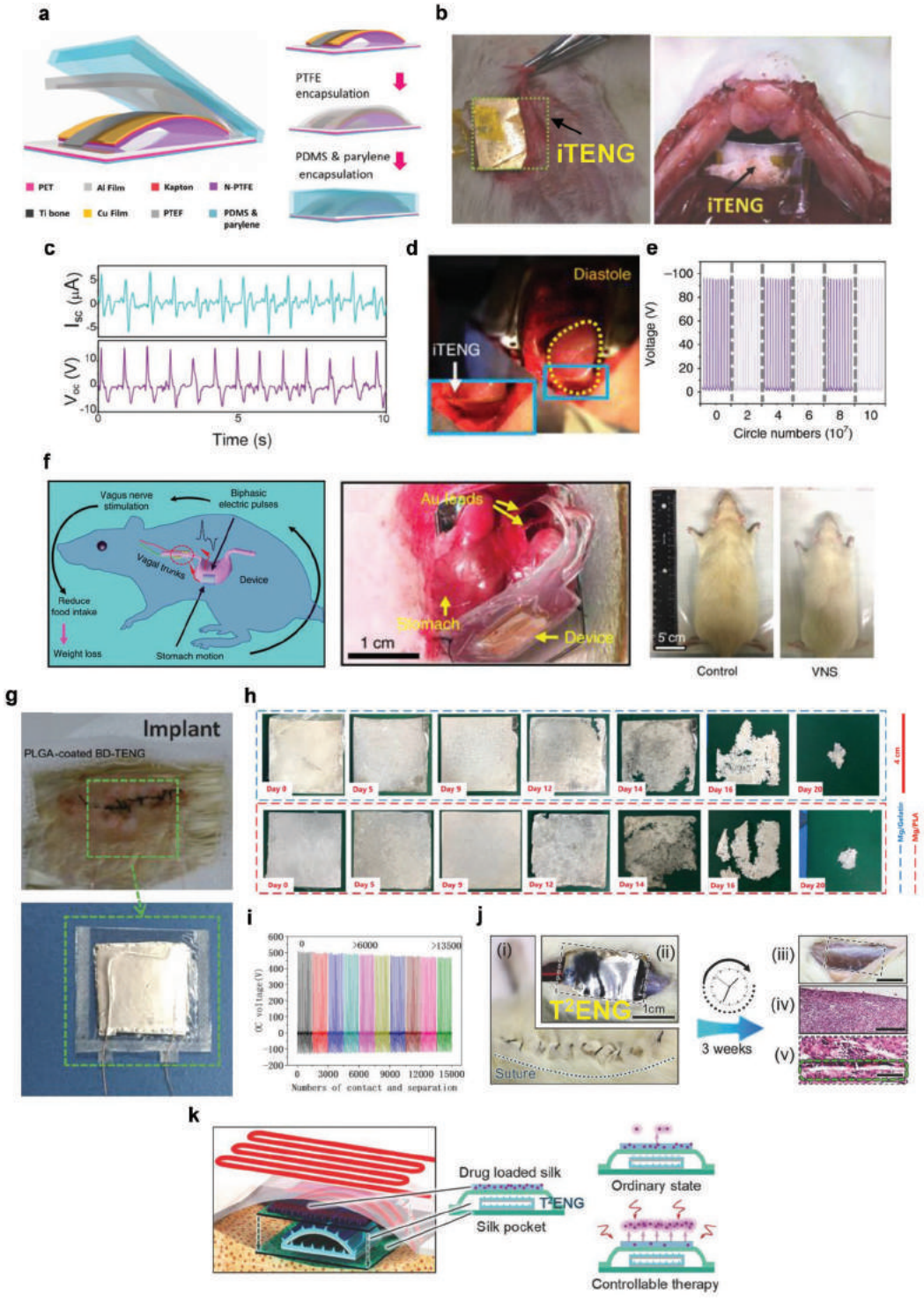

Figure 7. Triboelectric devices as power sources for implantable bioelectronics. a) A stacked arch-shaped structure of TENG. Reproduced with permission.[139] Copyright 2016, American Chemical Society. b) An implantable pacemaker powered by a flexible TENG. Reproduced with permission.[134] Copyright 2014, Wiley-VCH. c) In vivo output performance of a TENG in an adult Yorkshire Porcine. Reproduced with permission.[139] Copyright 2016, American Chemical Society. d) In vivo energy harvesting process driven by the diastole and systole of the heart. e) Stability performance of TENG. Reproduced with permission.[136] Copyright 2019, Springer nature. f) A "smart" vagus nerve stimulation system powered by a flexible TENG to achieve weight control. Reproduced with permission.[141] Copyright 2018, Springer nature. g) A biodegradable TENG implanted in the subdermal dorsal region of a SD rat. Reproduced with permission.[142] Copyright 2016, Science Advances. h) The degradation process of a fully biodegradable TENG. i) Stability of the TENG. Reproduced with permission.[143] Copyright 2017, Elsevier. j) A T^2ENG in the subdermal dorsal region of a SD rat. k) The schematic of a T^2ENG integrated with phenobarbital-doped silk film for "smart" drug release. Reproduced with permission.[119] Copyright 2018, Wiley-VCH.

and encapsulations layers; and dissolvable metals, such as Mg, acting as the electrodes.[119,142–144]

A biodegradable TENG composed of PLGA, PHV/B, PVA, PCL, and Mg in a multilayer structure has been reported. Tunable electrical output capabilities and degradation properties are achieved by fabricated TENG with different material combinations. The electrical output performance of the device can reach an open-circuit voltage of up to 40 V and a corresponding short-circuit current of 1 μA. Figure 7g shows the image of the implanted TENG located in the subdermal dorsal region of a Sprague–Dawley (SD) rat. Most constituent materials successfully biodegrade in the animal body within 9 weeks of implantation.[142] By introducing optimized gelatin and PLA as the triboelectric materials, a biodegradable TENG with improved power output is achieved (open circuit voltage of 500 V, short circuit current density of 10 mA m^{-2} and power density over 5 W cm^{-2} with a size of 4 × 4 cm), comparable to those made of nonbiodegradable materials. The constituent materials of TENG (Mg/gelatin and Mg/PLA) are fully degradable in water after 40 days, and the degradation process at various stages are illustrated in Figure 7h. In terms of mechanical reliability and stability, the output voltage of this TENG decreases slowly from 505 to 468 V after 15 000 cyclic contacts, as shown in Figure 7i.[143] Moreover, a multifunctional implantable transient triboelectric nanogenerator (T^2ENG) with real-time in vivo monitoring and "smart" treatment via controllable drug delivery has also been demonstrated. Figure 7j shows the image of the implanted T^2ENG with silk and Mg film as the triboelectric layers in the subdermal dorsal region of an SD mouse. The schematic of the T^2ENG integrated with the phenobarbital-doped silk film for "smart" drug release is illustrated in Figure 7k. The open-circuit voltage and the short-circuit current are 60 V and 1 μA, respectively, and the device is fully degradable.[119]

4.5. Thermoelectric Devices

Apart from mechanical motions, temperature gradients generated in the human body are another source of energy that can be harvested. The thermoelectric power generator (TEG) that converts heat energy to electric current based on Seebeck effects has been widely investigated.[145–147] The effectiveness of a thermoelectric material is determined by the dimensionless thermoelectric figure of merit, defined as $ZT = S^2\sigma T/\kappa$, where S, σ, T, and κ are the Seebeck coefficient, electrical conductivity, temperature, and thermal conductivity, respectively.[148,149] The performance of TEGs depends on the available temperature gradients, materials properties and device structure. Semiconductor materials such as bismuth telluride (Bi_2Te_3) and antimony telluride (Sb_2Te_3) are promising candidates for TEGs due to their large Seebeck coefficients.[150–153] Although conducting polymers including polyaniline, epoxy, polyimide (PI), polypyrrole, and poly (3,4-ethylenedioxythiophene:poly(styrenesulfonate)) have been proposed to fabricate flexible TEGs,[147,154–156] their output power density is not sufficient due to their low ZT values and high contact resistance. In order to achieve higher output power density and suppress the heat-loss through the substrates, organic–inorganic hybrid composite materials and associated coiled-up structures have been proposed as alternatives for fabricating flexible TEGs.[146,147,157–159] Nevertheless, the key challenge of the devices is to achieve sufficient temperature differences in physiological environments at the microscale.

A typical implanting configuration for TEG is to embed the device under the skin. So as to directly utilize the available thermal gradients. Based on the theoretical analysis, it is suggested that the best place for implanting a TEG is near the superficial skin, due to the maximum temperature differences present. In vitro experiments of a commercial TEG (TEC-01706T125, 15 × 15 × 3.9 mm) on the skin surface of a piece of pork (80 × 80 × 80 mm) is performed. A copper sheet placed underneath the tissue layer is connected with a thermostat water bath at 37 °C and the skin surface layer is exposed to the room environment to simulate the thermal status of the human body. The results show that the temperature gradient is stabilized at 0.5 K; the output voltage reaches around 3.3 mV before applying external cooling, where the thermal gradient approaches 1.1 K, and the TEG output voltage reaches 6 mV after the skin surface is cooled by ice. To further demonstrate the application of implanted TEGs for power harvesting, in vivo experiments are performed with rabbits (2 kg in size). A stable temperature gradient of 1.3 K is realized and the output voltage reaches 5 mV after implanting the TEG into the abdomen for 260 s. In contrast, after the skin surface is covered with an ice water bag, the temperature difference and the output voltage increase rapidly to 5.5 K and 25 mV, respectively.[160]

5. Energy Transfer Devices Utilize Sources from the Surrounding Environment

5.1. Ultrasonic Energy Harvesters

Compared to the energy harvesting from the human body, such as organ movements and thermal gradients, energy transferred from external sources could supply stable and adaptable power for implantable electronics. The ultrasonic driven wireless charging technology is an attractive method to energize implanted devices due to its advantages in safety, omnidirectionality, higher efficiencies at larger distances, and smaller device size.[161,162] The wavelength of ultrasound is critical to ensure both the resolution and penetration depth. The ultrasonic energy harvester is based on vibration, or sound waves, which can operate through either capacitance mode or piezoelectric mode.[163–165] The ultrasonic energy harvesters generally utilize piezoelectric transducers to convert mechanical vibrations induced by acoustic waves into electrical power, in order to achieve a desirable power level for in vivo applications. In order to develop implantable and flexible piezoelectric ultrasonic energy harvesters (PUEH), associated materials in the thin-film format have been investigated, including: PZT, sol–gel PZT, and epoxy for piezoelectric composites,[65,166–168] Cu and Au as interconnects,[65,166] PI and PDMS for substrates and encapsulations.[65,166,167] Conventional bioimplanted piezoelectric ultrasonic energy harvesters focus on the plate architecture because of its high theoretical acoustic power output. Diaphragm architecture has also been proposed to ensure conformal contact with the nonplanar surfaces of tissues and organs, generating more power than the plate architecture

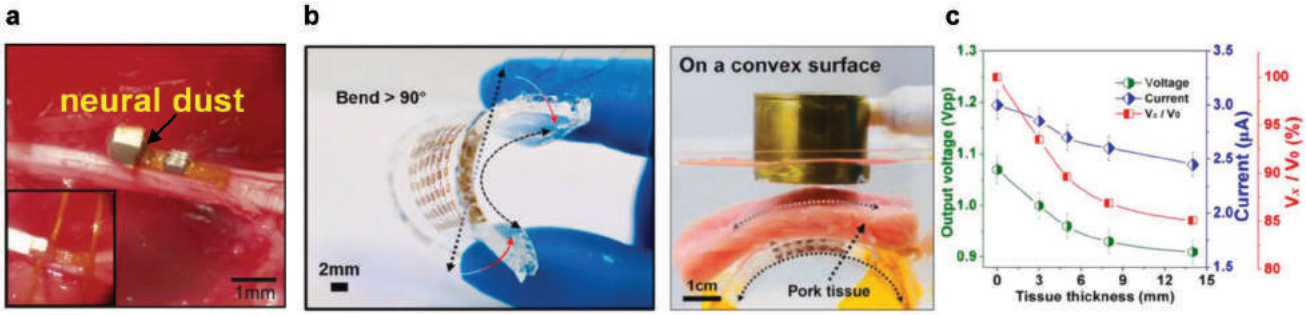

Figure 8. Ultrasonic energy harvesters as power sources for implantable bioelectronics. a) A neural dust system in a rat. Reproduced with permission.[169] Copyright 2016, Elsevier. b) The flexible property of the ultrasonic energy harvester (left) and the in vitro experiments of the ultrasonic energy harvester device on concave–convex surfaces (right). c) Output voltage under different tissue thickness. Reproduced with permission.[166] Copyright 2018, Elsevier.

and lowered sensitivity to changes in implantation depth and absorption power losses for sub-millimeter size devices.[164]

Figure 8a shows the first in vivo experiment of a neural dust system delivering power to mm-scale devices in the peripheral nervous system (PNS) of rats, recording the electroneurogram (ENG) from the sciatic nerve. The neural dust system consists of an external ultrasonic transceiver board, a piezoelectric crystal, a single custom transistor and a pair of recording electrodes, in which the piezocrystal converts the mechanical power of the transmitted external ultrasonic waves into electrical power for the transistor. Though the harvested power depends on the specifications of an external ultrasonic transducer, the efficiency of the neural dust when converting acoustic power to electrical power is about 25% on axis.[169] Further, an ultrasonically powered implanted microoxygen generator (IMOG) has been demonstrated.[170] However, both the neural dust and the IMOG power harvester are rigid and cannot be applied to soft and curvilinear surfaces. A flexible piezoelectric ultrasonic energy harvester capable of producing continuous power on both planar and curved surfaces is therefore designed and fabricated using PZT thin-films and wavy Cu interconnects encased in PDMS. The electrical power harvested is about 40 nW. Figure 8b shows the flexible properties of ultrasonic energy harvesters and the in vitro experiments of the device on concave–convex surfaces, mimicking the implanted situations. An output peak-to-peak voltage and current more than 2 Vpp and 4 μA is achieved. To mimic the different depth in the implanted tissue, different thicknesses of pork tissue (0–14 mm) were employed. The results show that there is no significant decrease in the output signals with the increased thickness of the inserted pork (Figure 8c).[166] All in all, although ultrasound is widely used for imaging at many centimeters of depth in the body, ultrasound energy harvesting for powering implantable electronics still needs to solve the significant issues of scattering and coupling of acoustic signals at the tissue interface before it can be widely applied.

5.2. Inductive Coupling/RF Energy Harvesters

Inductive coupling systems based on the mutual inductance between transmitter coils outside the body and receiver coils implanted in the body are widely adopted in IMDs for near-field wireless data transfer and energy harvesting.[4,171,172] As the external antenna transmits a varying electromagnetic signal near the skin, a voltage is generated by induction in the implanted receiver coils. The resonance frequency, distance, alignment, and mutual electromagnetic coupling between the transmitter and the receiver coils play a critical role in the energy transfer efficiency.[173–178] On the other hand, RF energy transfer represents far-field or midfield wireless energy harvesting options for implantable electronics. The stability and transfer efficiency depend on the field distribution of the electromagnetic waves and therefore the antenna design is critical to ensure preferential radiation direction alignment with the implantable devices. Nevertheless, heating issues, penetration depth, and appropriate antenna size are critical challenges to be overcome.[179–181]

In order to achieve miniaturized flexible inductive coupling or RF energy harvesting devices, an island structure of active electrical components, bridged with serpentine interconnects, or multilayer stacked structures integrated on soft substrates is generally adopted.[8,48,182] Biodegradable power harvesters can also be achieved by introducing biodegradable materials, including silicon nanomembranes (Si NMs) for the semiconductors, dissolvable metals (Mg, Mo) for the interconnects, MgO and SiO_2 for the dielectrics, and silk and PLGA for the substrates.[8,39,183]

An implanted miniaturized flexible RF power transfer device for wireless optogenetics is realized by connecting active electrical components with serpentine Ti/Au interconnecting thin-films embedded in a low-modulus PDMS elastomer. By designing the antenna to be flexible and stretchable, a device area of only 3 × 3 mm is needed when it is operated at 2.34 GHz—100 times smaller in volume and weight than those of conventional rigid antennas—as shown in **Figure 9**a. The mechanical stability is investigated, with the results showing that these devices can cycle $>10^5$ times without a detectable loss in optical power (Figure 9b).[8] The demonstrated system has the soft and stretchable features that can adapt anatomical shapes and natural motions, and can be used to modulate peripheral and spinal pain circuitry.

For biodegradable systems, a biodegradable full wave rectifying system, wirelessly powered by an RF transmitter and a Mg receiving antenna, is reported. The results show that the entire system initially disintegrates owing to the dissolution of the silk

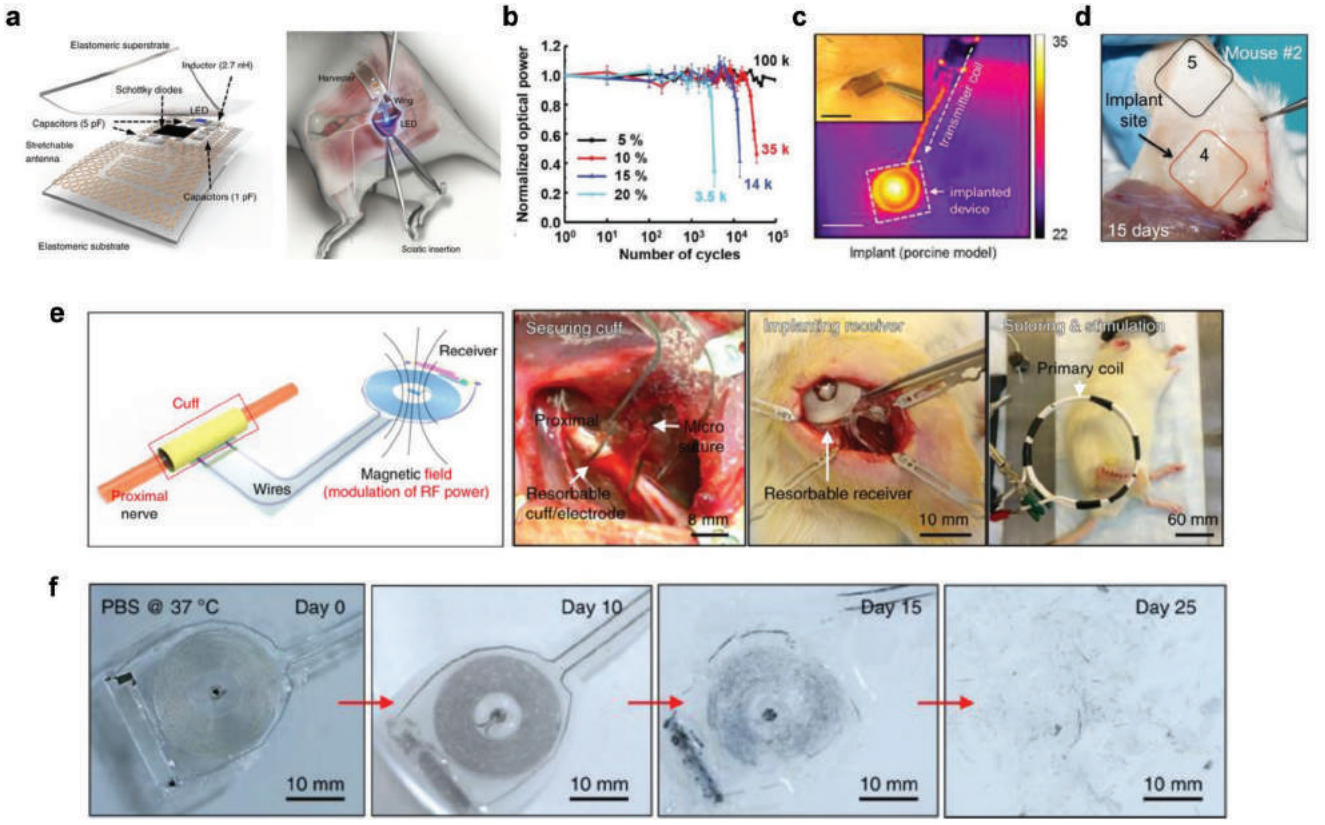

Figure 9. Conductive coupling/RF energy harvesters as power sources for implantable bioelectronics. a) An implanted flexible RF power transfer system. b) Optical output performance under the cyclical application of strain. Reproduced with permission.[8] Copyright 2015, Springer Nature. c) The thermal images of the wirelessly activated device in a porcine. Reproduced with permission.[184] Copyright 2015, Springer Nature. d) Devices examined after 15 days of implantation. Reproduced with permission.[185] Copyright 2014, National Academy of Sciences. e) Device structure and the surgical procedure of implanting the neural cuff to the sciatic nerve. f) The dissolution process of the bioresorbable wireless stimulator at various stages in PBS at 37° C. Reproduced with permission.[32] Copyright 2018, Springer Nature.

substrate followed by the other constituent materials, which dissolve at different rates.[183] In addition, a biodegradable and implantable drug delivery system with the ability to precisely release drugs upon external triggering by inductive coupling is demonstrated. Figure 9c gives the thermal image of the wirelessly activated device in a porcine model. It is reported that the release of the drug is only excited upon wireless electrical stimulus and no off-state leakage is visible for 24 h after implantation. The dissolution of the device begins from the interconnect parts after it is immersed in PBS (pH 7.4) at 37 °C for 1 week.[184] Moreover, a fully degradable, remotely controlled and implantable therapeutic device activated by inductive coupling is demonstrated. The in vivo experiments suggest that the device is fully degraded, with no visible residue, in 15 days, as presented in Figure 9d.[185]

Furthermore, a bioresorbable, implantable wireless stimulator, powered by a power harvester based on inductive coupling, for the peripheral nervous system is successfully created. Figure 9e presents the device structure and the surgical procedure of implanting the cuff to the sciatic nerve and implanting the inductive coupling harvester to subcutaneous tissue. The harvester consists of a loop antenna (Mg film), a dielectric interlayer (PLGA), a diode, and a capacitor. The results show that the output voltage can reach 100–300 mV at a distance of up to 80 mm. Testing of nerve repair shows that electrical stimulation, activated by the biodegradable inductive coupling system, may supply an enhanced rate of axonal regeneration and reduce the time for muscle reinnervation. The dissolution of the bioresorbable wireless stimulator after immersion for different time periods in PBS at 37 °C is shown in Figure 9f. The results illustrate that all the constituent materials completely disappear within 25 days.[32]

5.3. Photovoltaic Devices

Photovoltaics (PV) operating via a process of converting light directly into electricity using semiconductors. With years of effort, PV cells (or solar cells) have reached high photoconversion efficiency: over 26% for single junction silicon cells,[186] giving them a wide range of applications, even serving as implantable energy harvesters in biomedical systems. Being different from the conventional PV cells that operate in ambient and collect light energy without any optical block under normal circumstances, the implanted subcutaneous PV cells are enfolded in biological tissues, such as skins, fats, muscles and so forth. Nevertheless, the biological tissues still provide a means of photoelectric conversion with two optical transparency windows in the near-infrared (NIR) spectral region,

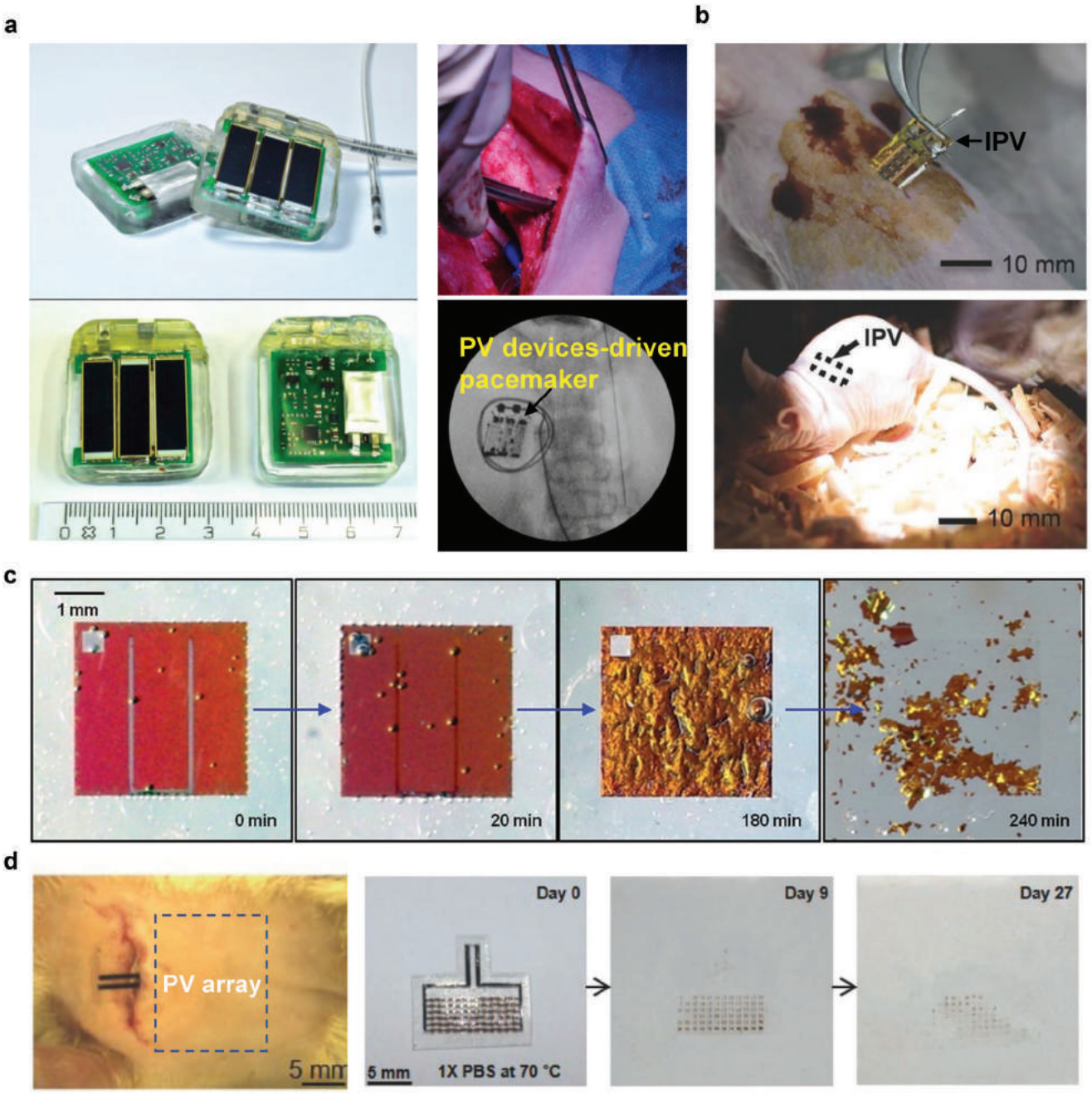

Figure 10. PV systems as power sources for implantable bioelectronics. a) Images of a PV cell-driven pacemaker (left) and subcutaneous implantation in pig (right). Reproduced with permission.[193] Copyright 2015, Elsevier. b) Surgical procedure to implant a PV device under the back skin of a hairless mouse (top), and a live hairless mouse model after implanted a PV device (bottom). Reproduced with permission.[194] Copyright 2016, Wiley-VCH. c) Various stages of the dissolution of a thin a-Si:H solar cell. Reproduced with permission.[42] Copyright 2015, American Chemical Society. d) Application of PV cells in rats and the accelerated dissolution test of a bioresorbable PV array in PBS solution. Reproduced with permission.[195] Copyright 2018, Wiley-VCH.

650–950 and 1000–1350 nm, respectively.[187,188] Furthermore, the PV cells hold efficient photoconversion in the NIR region with external quantum efficiency (EQE) approaching 100%, which is utilized in many high power conversion efficiency solar cells.[189] Based on this, PV cell energy harvesters applied to implantable biomedical electronics have attracted considerable interest during the past decades.

After the first demonstration of a photovoltaic wireless power supply for implanted cardiac pacemaker by Murakawa et al.,[190] extensive studies have been carried out on the potential exploitation of PV cells as wireless power solutions for implantable bioelectronics, including neural devices, retinal prosthesis, etc.[191,192] A modified battery-less pacemaker (30 × 35 × 6 mm) powered by solar modules (three monocrystalline silicon solar

Table 2. The advantages and disadvantages of different types of power devices.

Categories	Advantages	Disadvantages
Batteries	High energy density, cyclic stability, easy deployment	Large size, limited lifetime
Supercapacitors	Fast charge/discharge rates, high cycle lifetime, high power density	Low energy density
Biofuel cells	Abundant fuels in the body, good biocompatibility	Limited service life, low output power
Devices utilize biopotentials	Existing in the human body	Low output power
Piezoelectric harvesters	High output voltage, simple structure	Large size, biocompatibility issues of PZT, Limited implantable locations
Triboelectric devices	High output voltage, simple structure	Large size, limited implantable locations
Thermoelectric devices	Long-term energy supply	Low output power, low thermal gradient, limited implantable locations
Ultrasonic energy harvesters	Long-term energy supply, high efficiency	Low output power, orientation and coupling issues of acoustic signals
Inductive coupling/RF harvesters	Long-term energy supply, high output power	Large size, limited implantable depth, potential heating issues
Photovoltaic devices	Long-term energy supply, high output power	Large size, limited implantation depth

cells connected in series) has been recently demonstrated by Haeberlin et al.,[193] as shown in **Figure 10**a. The solar modules continue to yield an output power of about 6700 μW cm^{-2}, with an implantation depth of 2.4 mm in the right lateral neck of a pig (Figure 10a, right). Song and co-workers presented a flexible, implantable, and ultrathin gallium indium phosphide (GaInP)/gallium arsenide (GaAs)-based dual-junction PV devices, which could harvest high level of energy in vivo (Figure 10b).[194] The PV cell arrays generated a short-circuit current density (J_{sc}) of 2.6 mA cm^{-2} and an open-circuit voltage (V_{oc}) value of 4.5 V under the skin of a hairless mouse under standard test conditions (AM1.5G, 100 mW cm^{-2}).

It is of note that the PV cell-based power supply systems introduced above are not biodegradable, so that their applications are limited in bioresorbable transient electronics, which are only suitable for temporary biological procedures, such as wound healing, nerve stimulation, and medical sensing, and then completely disappear via resorption by the body. Since silicon has been proved as the predominant biodegradable semiconductor material,[39] the fully biodegradable PV cell energy harvesters based on silicon membranes have been investigated.

Kang et al. have reported a fully degradable amorphous silicon (a-Si) transient thin-film solar cell, and the dissolution process at various stages of a thin film a-Si:H solar cell is given in Figure 10c.[42] The electrode layers consisting of ZnO and Mg, which dissolve in hours, followed by the complete dissolution of the a-Si films within several days due to their different hydrolytic properties. The first fully biodegradable silicon solar cells implemented in vivo have been studied by Lu et al.[195] The fabricated PV cell arrays generate 64.4 μW and have a V_{oc} value of 4.25 V when covered with both skin and fat, under an optical power density of 200 mW cm^{-2} from the NIR (780 nm) light-emitting diode (LED) (Figure 10d). In order to analyze their biodegradable properties, accelerated dissolution tests have been conducted after the PV cell arrays are integrated into a biodegradable poly(lactic-*co*-glycolicacid) (PLGA) substrate. The results show that the whole PV system mostly degrades by hydrolysis after 27 days. Finally, the researchers verify the feasibility of the PV cells system as a fully biodegradable, bioresorbable, and implantable power supply system in vivo. All of the results offer a promising solution for the challenges of in vivo power supply for bioresorbable electronic implants.

In short, flexible or biodegradable photovoltaic devices of the order of several hundreds of microns for implantable electronics have been achieved, however, the implantation regions are limited to a few millimeters of depth in the body due to the scattering and absorption of the light source as well as potential tissue heating problems.

6. Conclusions and Research Outlook

Recent developments in nonconventional miniaturized, flexible, or biodegradable power devices for implantable bioelectronics have been reviewed. Advances in materials chemistry (intrinsically soft, biodegradable, or composite materials) and device architectures (1D nanowires, thin film membranes or island-bridge structures, etc.) are essential in reformulating conventional power devices and achieving novel biocompatible systems that can better adapt to the curvilinear and soft nature of biological organisms, as well as bioresorbable capability for targeting temporary usage. Flexible and biodegradable batteries are of great interest, due to their high energy densities and easy deployment. Miniaturization and operational lifetime remain a challenge for employment of minimally invasive longer-term applications. Supercapacitors have fast charge/discharge rates but lower energy densities, and can complement other energy harvesting methods. Biofuel cells that utilize electrochemical energy of biochemicals inside the body could potentially offer sufficient capacity, provided biofuels are continuously available; however, flexible or bioresorbable systems with sufficient power density and stability are yet to be developed. A variety of novel soft and biodegradable piezoelectric or triboelectric

devices that harvest the mechanical energy inside the body have been proposed, and could potentially be used in certain locations, such as the heart, to continuously power microdevices, although further reduction in size would be desirable. On the other hand, progress in harvesting energy by thermoelectric generator is impeded by the limited availability of temperature gradients in physiological conditions, and the need for further investigation into biocompatible thermoelectric materials and associated novel structures. Harvesting biopotential readily available in the human body represents another interesting area to be explored. Energy transfer through inductive coupling, RF magnetic waves, infrared light or ultrasound promises longer-term energy supply with high power density in a controlled manner, which could be attractive in deploying personalized medicine that requires frequent interaction of medical staff with both the implanted device and the patient. However, due to tissue absorption and scattering, as well as several pertinent safety issues, these methods are only applicable to a certain depth, and emerging flexible and bioresorbable systems with smaller size still require further development. The comparison of different types of power devices are summarized in **Table 2**.

Overall, innovative reformulation schemes of established materials in parallel with development of new active materials are equally important to achieve future advanced power devices by leveraging the existing manufacturing technologies for near term clinical translation. Soft or biodegradable encapsulation materials represent another important type of materials critical to ensure robust performance and sufficient lifetime of the devices, as penetration of biofluids and/or oxygen could significant deteriorate the performance of power devices, which recently has attracted significant academic attention. Integration of materials promoting device/tissue affinity of implantable power devices would be critical to minimize potential irritations and the foreign body responses. Involvement of novel stimuli-responsive materials could endow power devices with smarter functions and allow interactions with the implanted systems in more versatile modes through external stimuli. Further miniaturization of power devices sets the limiting factor of the total size of the bioelectronics platforms, and devices with sizes as small as 100 μm could ensure minimally invasive or even injectable implantation. Although the trade-off between device size and operational characteristics remains a critical challenge, the development of future ultralow power implantable bioelectronics may help to relax the pressure for continual size reduction of power devices to a certain extent. Future emerging power devices are moving toward the scale of a few hundred of microns, with increased biocompatible features (flexible, stretchable, and even biodegradable), that can deliver sufficient continuous power supply in a controlled manner are the ultimate goal for implantable electronics. Although it remains a great challenge to find a universal solution that addresses the power issue of implanted bioelectronics in all the regions of the human body, advances that combine various power options would enable multifunctional platforms for versatile and novel diagnostic and therapeutic systems that can potentially improve human healthcare.

Acknowledgements

X.H. and L.W. contributed equally to this work. This work was supported by National Natural Science Foundation of China (NSFC) 51601103 (L.Y.), 1000 Youth Talents Program in China (L.Y.), and China Postdoctoral Science Foundation 2018M641341 (L.W.).

Conflict of Interest

The authors declare no conflict of interest.

Keywords

biodegradable, flexible, implantable bioelectronics, miniaturization, power supply

Received: May 31, 2019
Revised: August 20, 2019
Published online: September 12, 2019

[1] J. A. Rogers, *JAMA, J. Am. Med. Assoc.* **2015**, *313*, 561.
[2] P. M. Lee, Z. Xiong, J. Ho, *Bioelectron. Med.* **2018**, *1*, 201.
[3] S.-K. Kang, J. Koo, Y. K. Lee, J. A. Rogers, *Acc. Chem. Res.* **2018**, *51*, 988.
[4] P. Gutruf, J. A. Rogers, *Curr. Opin. Neurobiol.* **2018**, *50*, 42.
[5] H. Fang, K. J. Yu, C. Gloschat, Z. Yang, E. Song, C.-H. Chiang, J. Zhao, S. M. Won, S. Xu, M. Trumpis, Y. Zhong, S. W. Han, Y. Xue, D. Xu, S. W. Choi, G. Cauwenberghs, M. Kay, Y. Huang, J. Viventi, I. R. Efimov, J. A. Rogers, *Nat. Biomed. Eng.* **2017**, *1*, 0038.
[6] D.-H. Kim, J. Viventi, J. J. Amsden, J. Xiao, L. Vigeland, Y.-S. Kim, J. A. Blanco, B. Panilaitis, E. S. Frechette, D. Contreras, D. L. Kaplan, F. G. Omenetto, Y. Huang, K.-C. Hwang, M. R. Zakin, B. Litt, J. A. Rogers, *Nat. Mater.* **2010**, *9*, 511.
[7] D. Son, J. Lee, D. J. Lee, R. Ghaffari, S. Yun, S. J. Kim, J. E. Lee, H. R. Cho, S. Yoon, S. Yang, S. Lee, S. Qiao, D. Ling, S. Shin, J.-K. Song, J. Kim, T. Kim, H. Lee, J. Kim, M. Soh, N. Lee, C. S. Hwang, S. Nam, N. Lu, T. Hyeon, S. H. Choi, D.-H. Kim, *ACS Nano* **2015**, *9*, 5937.
[8] S. I. Park, D. S. Brenner, G. Shin, C. D. Morgan, B. A. Copits, H. U. Chung, M. Y. Pullen, K. N. Noh, S. Davidson, S. J. Oh, J. Yoon, K.-I. Jang, V. K. Samineni, M. Norman, J. G. Grajales-Reyes, S. K. Vogt, S. S. Sundaram, K. M. Wilson, J. S. Ha, R. Xu, T. Pan, T.-i. Kim, Y. Huang, M. C. Montana, J. P. Golden, M. R. Bruchas, R. W. Gereau, J. A. Rogers, *Nat. Biotechnol.* **2015**, *33*, 1280.
[9] M. Bilitch, D. Escher, S. Furman, V. Parsonnet, *Am. J. Cardiol.* **1976**, *37*, 121.
[10] S. T. Lee, P. A. Williams, C. E. Braine, D.-T. Lin, S. W. M. John, P. P. Irazoqui, *IEEE Trans. Neural Syst. Rehabil. Eng.* **2015**, *23*, 655.
[11] L. Han, X. Lu, M. Wang, D. Gan, W. Deng, K. Wang, L. Fang, K. Liu, C. W. Chan, Y. Tang, L.-T. Weng, H. Yuan, *Small* **2017**, *13*, 1601916.
[12] L. Han, K. Liu, M. Wang, K. Wang, L. Fang, H. Chen, J. Zhou, X. Lu, *Adv. Funct. Mater.* **2018**, *28*, 1704195.
[13] L. Han, L. Yan, K. Wang, L. Fang, H. Zhang, Y. Tang, Y. Ding, L.-T. Weng, J. Xu, J. Weng, Y. Liu, F. Ren, X. Lu, *NPG Asia Mater.* **2017**, *9*, e372.
[14] L. Han, L. Yan, M. Wang, K. Wang, L. Fang, J. Zhou, J. Fang, F. Ren, X. Lu, *Chem. Mater.* **2018**, *30*, 5561.

[15] Y. Zhang, C.-H. Chen, T. He, G. C. Temes, *IEEE J. Solid-State Circuits* **2017**, *52*, 1066.
[16] Y.-S. Shu, L.-T. Kuo, T.-Y. Lo, *IEEE J. Solid-State Circuits* **2016**, *51*, 2928.
[17] M. Cai, Z. Wang, Y. Luo, S. Mirabbasi, *IEEE Trans. Microwave Theory Tech.* **2018**, *66*, 5129.
[18] M. Zgaren, A. Moradi, L.-F. Tanguay, M. Sawan, *Int. J. Circuit Theory Appl.* **2018**, *46*, 2266.
[19] L. S. Y. Wong, S. Hossain, A. Ta, J. Edvinsson, D. H. Rivas, H. Naas, *IEEE J. Solid-State Circuits* **2004**, *39*, 2446.
[20] J. T. Heaton, J. B. Kobler, D. M. Otten, R. E. Hillman, S. M. Zeitels, *Ann. Otol., Rhinol. Laryngol.* **2019**, *128*, 53S.
[21] A. Bansal, F. Yang, T. Xi, Y. Zhang, J. S. Ho, *Proc. Natl. Acad. Sci. USA* **2018**, *115*, 1469.
[22] B. Fan, K. Y. Kwon, A. J. Weber, W. Li, in *2014 36th Annual Int. Conf. of the IEEE Engineering in Medicine and Biology Society*, IEEE, Chicago, IL, USA **2014**, p. 450.
[23] Y. Nishio, A. Kobayashi, K. Niitsu, *IEICE Trans. Electron.* **2019**, *E102.C*, 269.
[24] Y. Lee, B. Giridhar, Z. Foo, D. Sylvester, D. B. Blaauw, *IEEE J. Solid-State Circuits* **2013**, *48*, 2511.
[25] H. Basaeri, Y. Yu, D. Young, S. Roundy, *IEEE Sens. Lett.* **2019**, *3*, 1.
[26] A. Sawaby, M. L. Wang, E. So, J.-C. Chien, H. Nan, B. T. Khuri-Yakub, A. Arbabian, in *2018 IEEE Symp. on VLSI Circuits*, IEEE, Honolulu, HI, USA **2018**, p. 189.
[27] V. Sivaji, D. W. Grasse, S. A. Hays, J. E. Bucksot, R. Saini, M. P. Kilgard, R. L. RennakerII, *J. Neurosci. Methods* **2019**, *320*, 26.
[28] H. Kang, W. H. Abbasi, S.-W. Kim, J. Kim, *Sensors* **2019**, *19*, 536.
[29] S. Anand, J. Sutanto, M. S. Baker, M. Okandan, J. Muthuswamy, *J. Microelectromech. Syst.* **2012**, *21*, 1172.
[30] V. R. Feig, H. Tran, Z. Bao, *ACS Cent. Sci.* **2018**, *4*, 337.
[31] C. M. Boutry, Y. Kaizawa, B. C. Schroeder, A. Chortos, A. Legrand, Z. Wang, J. Chang, P. Fox, Z. Bao, *Nat. Electron.* **2018**, *1*, 314.
[32] J. Koo, M. R. MacEwan, S.-K. Kang, S. M. Won, M. Stephen, P. Gamble, Z. Xie, Y. Yan, Y.-Y. Chen, J. Shin, N. Birenbaum, S. Chung, S. B. Kim, J. Khalifeh, D. V. Harburg, K. Bean, M. Paskett, J. Kim, Z. S. Zohny, S. M. Lee, R. Zhang, K. Luo, B. Ji, A. Banks, H. M. Lee, Y. Huang, W. Z. Ray, J. A. Rogers, *Nat. Med.* **2018**, *24*, 1830.
[33] L. Yin, X. Huang, H. Xu, Y. Zhang, J. Lam, J. Cheng, J. A. Rogers, *Adv. Mater.* **2014**, *26*, 3879.
[34] X. Huang, D. Wang, Z. Yuan, W. Xie, Y. Wu, R. Li, Y. Zhao, D. Luo, L. Cen, B. Chen, H. Wu, H. Xu, X. Sheng, M. Zhang, L. Zhao, L. Yin, *Small* **2018**, *14*, 1800994.
[35] G. D. Cha, D. Kang, J. Lee, D.-H. Kim, *Adv. Healthcare Mater.* **2019**, *8*, 1801660.
[36] R. Li, L. Wang, L. Yin, *Materials* **2018**, *11*, 2108.
[37] R. Li, L. Wang, D. Kong, L. Yin, *Bioactive Mater.* **2018**, *3*, 322.
[38] S.-W. Hwang, G. Park, H. Cheng, J.-K. Song, S.-K. Kang, L. Yin, J.-H. Kim, F. G. Omenetto, Y. Huang, K.-M. Lee, J. A. Rogers, *Adv. Mater.* **2014**, *26*, 1992.
[39] S.-W. Hwang, H. Tao, D.-H. Kim, H. Cheng, J.-K. Song, E. Rill, M. A. Brenckle, B. Panilaitis, S. M. Won, Y.-S. Kim, Y. M. Song, K. J. Yu, A. Ameen, R. Li, Y. Su, M. Yang, D. L. Kaplan, M. R. Zakin, M. J. Slepian, Y. Huang, F. G. Omenetto, J. A. Rogers, *Science* **2012**, *337*, 1640.
[40] Y.-H. Zou, J. Wang, L.-Y. Cui, R.-C. Zeng, Q.-Z. Wang, Q.-X. Han, J. Qiu, X.-B. Chen, D.-C. Chen, S.-K. Guan, Y.-F. Zheng, *Acta Biomater.*https://doi.org/10.1016/j.actbio.2019.05.069.
[41] D. She, M. Tsang, M. Allen, *Biomed. Microdevices* **2019**, *21*, 17.
[42] S.-K. Kang, G. Park, K. Kim, S.-W. Hwang, H. Cheng, J. Shin, S. Chung, M. Kim, L. Yin, J. C. Lee, K.-M. Lee, J. A. Rogers, *ACS Appl. Mater. Interfaces* **2015**, *7*, 9297.
[43] S. H. Jin, S.-K. Kang, I.-T. Cho, S. Y. Han, H. U. Chung, D. J. Lee, J. Shin, G. W. Baek, T.-i. Kim, J.-H. Lee, J. A. Rogers, *ACS Appl. Mater. Interfaces* **2015**, *7*, 8268.
[44] L. Wang, Y. Gao, F. Dai, D. Kong, H. Wang, P. Sun, Z. Shi, X. Sheng, B. Xu, L. Yin, *ACS Appl. Mater. Interfaces* **2019**, *11*, 18013.
[45] Z. Li, G. Zhu, R. Yang, A. C. Wang, Z. L. Wang, *Adv. Mater.* **2010**, *22*, 2534.
[46] D.-H. Kim, N. Lu, R. Ghaffari, Y.-S. Kim, S. P. Lee, L. Xu, J. Wu, R.-H. Kim, J. Song, Z. Liu, J. Viventi, B. de Graff, B. Elolampi, M. Mansour, M. J. Slepian, S. Hwang, J. D. Moss, S.-M. Won, Y. Huang, B. Litt, J. A. Rogers, *Nat. Mater.* **2011**, *10*, 316.
[47] K. Nan, S. D. Kang, K. Li, K. J. Yu, F. Zhu, J. Wang, A. C. Dunn, C. Zhou, Z. Xie, M. T. Agne, H. Wang, H. Luan, Y. Zhang, Y. Huang, G. J. Snyder, J. A. Rogers, *Sci. Adv.* **2018**, *4*, eaau5849.
[48] P. Gutruf, V. Krishnamurthi, A. Vázquez-Guardado, Z. Xie, A. Banks, C.-J. Su, Y. Xu, C. R. Haney, E. A. Waters, I. Kandela, S. R. Krishnan, T. Ray, J. P. Leshock, Y. Huang, D. Chanda, J. A. Rogers, *Nat. Electron.* **2018**, *1*, 652.
[49] W. Greatbatch, C. F. Holmes, *IEEE Eng. Med. Biol. Mag.* **1991**, *10*, 38.
[50] H. Jimbo, N. Miki, *Sens. Actuators, B* **2008**, *134*, 219.
[51] P. Nadeau, D. El-Damak, D. Glettig, Y. L. Kong, S. Mo, C. Cleveland, L. Booth, N. Roxhed, R. Langer, A. P. Chandrakasan, G. Traverso, *Nat. Biomed. Eng.* **2017**, *1*, 0022.
[52] X. Jia, Y. Yang, C. Wang, C. Zhao, R. Vijayaraghavan, D. R. MacFarlane, M. Forsyth, G. G. Wallace, *ACS Appl. Mater. Interfaces* **2014**, *6*, 21110.
[53] H. Hafezi, T. L. Robertson, G. D. Moon, K.-Y. Au-Yeung, M. J. Zdeblick, G. M. Savage, *IEEE Trans. Biomed. Eng.* **2015**, *62*, 99.
[54] X. Jia, C. Wang, V. Ranganathan, B. Napier, C. Yu, Y. Chao, M. Forsyth, F. G. Omenetto, D. R. MacFarlane, G. G. Wallace, *ACS Energy Lett.* **2017**, *2*, 831.
[55] G. Liu, J. Y. Kim, M. Wang, J.-Y. Woo, L. Wang, D. Zou, J. K. Lee, *Adv. Energy Mater.* **2018**, *8*, 1703652.
[56] R. Guo, J. Liu, *J. Micromech. Microeng.* **2017**, *27*, 104002.
[57] M. Tsang, A. Armutlulu, A. W. Martinez, S. A. B. Allen, M. G. Allen, *Microsyst. Nanoeng.* **2015**, *1*, 15024.
[58] M. Tsang, A. Armutlulu, A. Martinez, F. Herrault, S. A. B. Allen, M. G. Allen, in *2014 IEEE 27th Int. Conf. on MEMS*, IEEE, San Francisco, CA, USA **2014**, p. 358.
[59] Y. J. Kim, S.-E. Chun, J. Whitacre, C. J. Bettinger, *J. Mater. Chem. B* **2013**, *1*, 3781.
[60] Y. J. Kim, W. Wu, S.-E. Chun, J. F. Whitacre, C. J. Bettinger, *Proc. Natl. Acad. Sci. USA* **2013**, *110*, 20912.
[61] Y. J. Kim, A. Khetan, W. Wu, S.-E. Chun, V. Viswanathan, J. F. Whitacre, C. J. Bettinger, *Adv. Mater.* **2016**, *28*, 3173.
[62] Y. J. Kim, W. Wu, S.-E. C. hun, J. F. Whitacre, C. J. Bettinger, *Adv. Mater.* **2014**, *26*, 6572.
[63] D. L. Robinson, A. Hermans, A. T. Seipel, R. M. Wightman, *Chem. Rev.* **2008**, *108*, 2554.
[64] T. Sun, Z.-J. Li, H.-G. Wang, D. Bao, F.-L. Meng, X.-B. Zhang, *Angew. Chem.* **2016**, *128*, 10820; *Angew. Chem., Int. Ed.* **2016**, *55*, 10662.
[65] H. Wang, P. Hu, J. Yang, G. Gong, L. Guo, X. Chen, *Adv. Mater.* **2015**, *27*, 2348.
[66] G. Lee, S.-K. Kang, S. M. Won, P. Gutruf, Y. R. Jeong, J. Koo, S.-S. Lee, J. A. Rogers, J. S. Ha, *Adv. Energy Mater.* **2017**, *7*, 1700157.
[67] H. Li, C. Zhao, X. Wang, J. Meng, Y. Zou, S. Noreen, L. Zhao, Z. Liu, H. Ouyang, P. Tan, M. Yu, Y. Fan, Z. L. Wang, Z. Li, *Adv. Sci.* **2019**, *6*, 1801625.
[68] F. Thissandier, P. Gentile, T. Brousse, G. Bidan, S. Sadki, *J. Power Sources* **2014**, *269*, 740.

[69] S. He, Y. Hu, J. Wan, Q. Gao, Y. Wang, S. Xie, L. Qiu, C. Wang, G. Zheng, B. Wang, H. Peng, *Carbon* **2017**, *122*, 162.
[70] Z. Zhang, J. Deng, X. Li, Z. Yang, S. He, X. Chen, G. Guan, J. Ren, H. Peng, *Adv. Mater.* **2015**, *27*, 356.
[71] Z. Yang, J. Deng, X. Chen, J. Ren, H. Peng, *Angew. Chem., Int. Ed.* **2013**, *52*, 13453.
[72] P. Xu, T. Gu, Z. Cao, B. Wei, J. Yu, F. Li, J.-H. Byun, W. Lu, Q. Li, T.-W. Chou, *Adv. Energy Mater.* **2014**, *4*, 1300759.
[73] P. Kumar, E. Di Mauro, S. Zhang, A. Pezzella, F. Soavi, C. Santato, F. Cicoira, *J. Mater. Chem. C* **2016**, *4*, 9516.
[74] X. Wang, W. Xu, P. Chatterjee, C. Lv, J. Popovich, Z. Song, L. Dai, M. Y. S. Kalani, S. E. Haydel, H. Jiang, *Adv. Mater. Technol.* **2016**, *1*, 1600059.
[75] J. S. Chae, N.-S. Heo, C. H. Kwak, W.-S. Cho, G. H. Seol, W.-S. Yoon, H.-K. Kim, D. J. Fray, A. T. E. Vilian, Y.-K. Han, Y. S. Huh, K. C. Roh, *Nano Energy* **2017**, *34*, 86.
[76] J. Hur, K. Im, S. W. Kim, U. J. Kim, J. Lee, S. Hwang, J. Song, S. Kim, S. Hwang, N. Park, *J. Mater. Chem. A* **2013**, *1*, 14460.
[77] H. J. Sim, C. Choi, D. Y. Lee, H. Kim, J.-H. Yun, J. M. Kim, T. M. Kang, R. Ovalle, R. H. Baughman, C. W. Kee, S. J. Kim, *Nano Energy* **2018**, *47*, 385.
[78] F. Qian, D. E. Morse, *Trends Biotechnol.* **2011**, *29*, 62.
[79] A. T. Yahiro, S. M. Lee, D. O. Kimble, *Biochim. Biophys. Acta* **1964**, *88*, 375.
[80] N. Mano, F. Mao, A. Heller, *J. Am. Chem. Soc.* **2002**, *124*, 12962.
[81] A. Heller, *Phys. Chem. Chem. Phys.* **2004**, *6*, 209.
[82] E. H. Yu, K. Scott, *Energies* **2010**, *3*, 23.
[83] T. Miyake, K. Haneda, N. Nagai, Y. Yatagawa, H. Onami, S. Yoshino, T. Abe, M. Nishizawa, *Energy Environ. Sci.* **2011**, *4*, 5008.
[84] V. Flexer, N. Mano, *Anal. Chem.* **2010**, *82*, 1444.
[85] M. Rasmussen, R. E. Ritzmann, I. Lee, A. J. Pollack, D. Scherson, *J. Am. Chem. Soc.* **2012**, *134*, 1458.
[86] K. Shoji, Y. Akiyama, M. Suzuki, N. Nakamura, H. Ohno, K. Morishima, *Biosens. Bioelectron.* **2016**, *78*, 390.
[87] L. Halámková, J. Halámek, V. Bocharova, A. Szczupak, L. Alfonta, E. Katz, *J. Am. Chem. Soc.* **2012**, *134*, 5040.
[88] A. Szczupak, J. Halámek, L. Halámková, V. Bocharova, L. Alfonta, E. Katz, *Energy Environ. Sci.* **2012**, *5*, 8891.
[89] K. MacVittie, J. Halámek, L. Halámková, M. Southcott, W. D. Jemison, R. Lobeld, E. Katz, *Energy Environ. Sci.* **2013**, *6*, 81.
[90] P. Cinquin, C. Gondran, F. Giroud, S. Mazabrard, A. Pellissier, F. Boucher, J.-P. Alcaraz, K. Gorgy, F. Lenouvel, S. Mathé, P. Porcu, S. Cosnier, *PLoS One* **2010**, *5*, e10476.
[91] S. El Ichi, A. Zebda, J.-P. Alcaraz, A. Laaroussi, F. Boucher, J. Boutonnat, N. Reverdy-Bruas, D. Chaussy, M. N. Belgacem, P. Cinquin, D. K. Martin, *Energy Environ. Sci.* **2015**, *8*, 1017.
[92] A. Zebda, S. Cosnier, J.-P. Alcaraz, M. Holzinger, A. Le Goff, C. Gondran, F. Boucher, F. Giroud, K. Gorgy, H. Lamraoui, P. Cinquin, *Sci. Rep.* **2013**, *3*, 1516.
[93] C. H. Kwon, Y. Ko, D. Shin, M. Kwon, J. Park, W. K. Bae, S. W. Lee, J. Cho, *Nat. Commun.* **2018**, *9*, 4479.
[94] F. C. P. F. Sales, R. M. Iost, M. V. A. Martins, M. C. Almeida, F. N. Crespilho, *Lab Chip* **2013**, *13*, 468.
[95] D. Desmaele, L. Renaud, S. Tingry, *Sens. Actuators, B* **2015**, *220*, 583.
[96] A. Zebda, J.-P. Alcaraz, P. Vadgama, S. Shleev, S. D. Minteer, F. Boucher, P. Cinquin, D. K. Martin, *Bioelectrochemistry* **2018**, *124*, 57.
[97] S. Kerzenmacher, J. Ducrée, R. Zengerle, F. von Stetten, *J. Power Sources* **2008**, *182*, 1.
[98] J. Giner, G. Holleck, P. A. Malachesky, *Ber. Bunsen-Ges.-Phys. Chem.* **1973**, *77*, 782.
[99] B. I. Rapoport, J. T. Kedzierski, R. Sarpeshkar, *PLoS One* **2012**, *7*, e38436.
[100] W. Jia, G. Valdés-Ramírez, A. J. Bandodkar, J. R. Windmiller, J. Wang, *Angew. Chem., Int. Ed.* **2013**, *52*, 7233.
[101] W. Jia, X. Wang, S. Imani, A. J. Bandodkar, J. Ramirez, P. P. Mercier, J. Wang, *J. Mater. Chem. A* **2014**, *2*, 18184.
[102] F. Alam, S. RoyChoudhury, A. H. Jalal, Y. Umasankar, S. Forouzanfar, N. Akter, S. Bhansali, N. Pala, *Biosens. Bioelectron.* **2018**, *117*, 818.
[103] R. L. Arechederra, K. Boehm, S. D. Minteer, *Electrochim. Acta* **2009**, *54*, 7268.
[104] J. Zhao, F. Meng, X. Zhu, K. Han, S. Liu, G. Li, *Electroanalysis* **2008**, *20*, 1593.
[105] D. Bhatnagar, S. Xu, C. Fischer, R. L. Arechederra, S. D. Minteer, *Phys. Chem. Chem. Phys.* **2011**, *13*, 86.
[106] P. P. Mercier, A. C. Lysaght, S. Bandyopadhyay, A. P. Chandrakasan, K. M. Stankovic, *Nat. Biotechnol.* **2012**, *30*, 1240.
[107] L. Catacuzzeno, F. Orfei, A. Di Michele, L. Sforna, F. Franciolini, L. Gammaitoni, *Nano Energy* **2019**, *56*, 823.
[108] T. B. H. Schroeder, A. Guha, A. Lamoureux, G. VanRenterghem, D. Sept, M. Shtein, J. Yang, M. Mayer, *Nature* **2017**, *552*, 214.
[109] X. Chen, S. Xu, N. Yao, Y. Shi, *Nano Lett.* **2010**, *10*, 2133.
[110] C. Dagdeviren, B. D. Yang, Y. Su, P. L. Tran, P. Joe, E. Anderson, J. Xia, V. Doraiswamy, B. Dehdashti, X. Feng, B. Lu, R. Poston, Z. Khalpey, R. Ghaffari, Y. Huang, M. J. Slepian, J. A. Rogers, *Proc. Natl. Acad. Sci. USA* **2014**, *111*, 1927.
[111] B. Lu, Y. Chen, D. Ou, H. Chen, L. Diao, W. Zhang, J. Zheng, W. Ma, L. Sun, X. Feng, *Sci. Rep.* **2015**, *5*, 16065.
[112] D. H. Kim, H. J. Shin, H. Lee, C. K. Jeong, H. Park, G.-T. Hwang, H.-Y. Lee, D. J. Joe, J. H. Han, S. H. Lee, J. Kim, B. Joung, K. J. Lee, *Adv. Funct. Mater.* **2017**, *27*, 1700341.
[113] C. Dagdeviren, S.-W. Hwang, Y. Su, S. Kim, H. Cheng, O. Gur, R. Haney, F. G. Omenetto, Y. Huang, J. A. Rogers, *Small* **2013**, *9*, 3398.
[114] Z. Li, R. Yang, M. Yu, F. Bai, C. Li, Z. L. Wang, *J. Phys. Chem. C* **2008**, *112*, 20114.
[115] C. K. Jeong, J. H. Han, H. Palneedi, H. Park, G.-T. Hwang, B. Joung, S.-G. Kim, H. J. Shin, I.-S. Kang, J. Ryu, K. J. Lee, *APL Mater.*. **2017**, *5*, 074102.
[116] H. Zhang, X.-S. Zhang, X. Cheng, Y. Liu, M. Han, X. Xue, S. Wang, F. Yang, A. S. Smitha, H. Zhang, Z. Xu, *Nano Energy* **2015**, *12*, 296.
[117] L. Xing, Y. Nie, X. Xue, Y. Zhang, *Nano Energy* **2014**, *10*, 44.
[118] Y. Yu, H. Sun, H. Orbay, F. Chen, C. G. England, W. Cai, X. Wang, *Nano Energy* **2016**, *27*, 275.
[119] A. Wang, Z. Liu, M. Hu, C. Wang, X. Zhang, B. Shi, Y. Fan, Y. Cui, Z. Li, K. Ren, *Nano Energy* **2018**, *43*, 63.
[120] X. Cheng, X. Xue, Y. Ma, M. Han, W. Zhang, Z. Xu, H. Zhang, H. Zhang, *Nano Energy* **2016**, *22*, 453.
[121] K. Maity, D. Mandal, *ACS Appl. Mater. Interfaces* **2018**, *10*, 18257.
[122] B. Y. Lee, J. Zhang, C. Zueger, W.-J. Chung, S. Y. Yoo, E. Wang, J. Meyer, R. Ramesh, S.-W. Lee, *Nat. Nanotechnol.* **2012**, *7*, 351.
[123] S. K. Ghosh, D. Mandal, *Nano Energy* **2016**, *28*, 356.
[124] M. Deterre, E. Lefeuvre, Y. Zhu, M. Woytasik, B. Boutaud, R. Dal Molin, *J. Microelectromech. Syst.* **2014**, *23*, 651.
[125] K. Heo, H.-E. Jin, H. Kim, J. H. Lee, E. Wang, S.-W. Lee, *Nano Energy* **2019**, *56*, 716.
[126] F.-R. Fan, Z.-Q. Tian, Z. L. Wang, *Nano Energy* **2012**, *1*, 328.
[127] F. R. Fan, W. Tang, Z. L. Wang, *Adv. Mater.* **2016**, *28*, 4283.
[128] X.-S. Zhang, M.-D. Han, R.-X. Wang, F.-Y. Zhu, Z.-H. Li, W. Wang, H.-X. Zhang, *Nano Lett.* **2013**, *13*, 1168.
[129] R. Hinchet, S.-W. Kim, *ACS Nano* **2015**, *9*, 7742.
[130] L. Dhakar, F. E. H. Tay, C. Lee, *J. Micromech. Microeng.* **2014**, *24*, 104002.
[131] L. Dhakar, P. Pitchappa, F. E. H. Tay, C. Lee, *Nano Energy* **2016**, *19*, 532.
[132] Z. L. Wang, *ACS Nano* **2013**, *7*, 9533.

[133] J. Ha, J. Chung, S.-M. Kim, J. H. Kim, S. Shin, J. Y. Park, S. Lee, J.-B. Kim, *Nano Energy* **2017**, *36*, 126.
[134] Q. Zheng, B. Shi, F. Fan, X. Wang, L. Yan, W. Yuan, S. Wang, H. Liu, Z. Li, Z. L. Wang, *Adv. Mater.* **2014**, *26*, 5851.
[135] G. Zhu, Y. S. Zhou, P. Bai, X. S. Meng, Q. Jing, J. Chen, Z. L. Wang, *Adv. Mater.* **2014**, *26*, 3788.
[136] H. Ouyang, Z. Liu, N. Li, B. Shi, Y. Zou, F. Xie, Y. Ma, Z. Li, H. Li, Q. Zheng, X. Qu, Y. Fan, Z. L. Wang, H. Zhang, Z. Li, *Nat. Commun.* **2019**, *10*, 1821.
[137] A. F. Diaz, R. M. Felix-Navarro, *J. Electrostat.* **2004**, *62*, 277.
[138] F.-R. Fan, L. Lin, G. Zhu, W. Wu, R. Zhang, Z. L. Wang, *Nano Lett.* **2012**, *12*, 3109.
[139] Q. Zheng, H. Zhang, B. Shi, X. Xue, Z. Liu, Y. Jin, Y. Ma, Y. Zou, X. Wang, Z. An, W. Tang, W. Zhang, F. Yang, Y. Liu, X. Lang, Z. Xu, Z. Li, Z. L. Wang, *ACS Nano* **2016**, *10*, 6510.
[140] W. Tang, B. Meng, H. X. Zhang, *Nano Energy* **2013**, *2*, 1164.
[141] G. Yao, L. Kang, J. Li, Y. Long, H. Wei, C. A. Ferreira, J. J. Jeffery, Y. Lin, W. Cai, X. Wang, *Nat. Commun.* **2018**, *9*, 5349.
[142] Q. Zheng, Y. Zou, Y. Zhang, Z. Liu, B. Shi, X. Wang, Y. Jin, H. Ouyang, Z. Li, Z. L. Wang, *Sci. Adv.* **2016**, *2*, e1501478.
[143] R. Pan, W. Xuan, J. Chen, S. Dong, H. Jin, X. Wang, H. Li, J. Luo, *Nano Energy* **2018**, *45*, 193.
[144] R. Wang, S. Gao, Z. Yang, Y. Li, W. Chen, B. Wu, W. Wu, *Adv. Mater.* **2018**, *30*, 1706267.
[145] A. Cadei, A. Dionisi, E. Sardini, M. Serpelloni, *Meas. Sci. Technol.* **2014**, *25*, 012003.
[146] S. J. Kim, J. H. We, B. J. Cho, *Energy Environ. Sci.* **2014**, *7*, 1959.
[147] J. Weber, K. Potje-Kamloth, F. Haase, P. Detemple, F. Völklein, T. Doll, *Sens. Actuators, A* **2006**, *132*, 325.
[148] J. He, M. G. Kanatzidis, V. P. Dravid, *Mater. Today* **2013**, *16*, 166.
[149] G. J. Snyder, E. S. Toberer, *Nat. Mater.* **2008**, *7*, 105.
[150] M. S. Dresselhaus, G. Chen, M. Y. Tang, R. G. Yang, H. Lee, D. Z. Wang, Z. F. Ren, J.-P. Fleurial, P. Gogna, *Adv. Mater.* **2007**, *19*, 1043.
[151] B. Poudel, Q. Hao, Y. Ma, Y. Lan, A. Minnich, B. Yu, X. Yan, D. Wang, A. Muto, D. Vashaee, X. Chen, J. Liu, M. S. Dresselhaus, G. Chen, Z. Ren, *Science* **2008**, *320*, 634.
[152] J. Li, Q. Tan, J.-F. Li, D.-W. Liu, F. Li, Z.-Y. Li, M. Zou, K. Wang, *Adv. Funct. Mater.* **2013**, *23*, 4317.
[153] Y. Pei, X. Shi, A. LaLonde, H. Wang, L. Chen, G. J. Snyder, *Nature* **2011**, *473*, 66.
[154] J. Liu, L.-m. Zhang, L. He, X.-f. Tang, *J. Wuhan Univ. Technol., Mater. Sci. Ed.* **2003**, *18*, 53.
[155] A. Eftekhari, M. Kazemzad, M. Keyanpour-Rad, *Polym. J.* **2006**, *38*, 781.
[156] A. M. Nardes, M. Kemerink, R. A. J. Janssen, J. A. M. Bastiaansen, N. M. M. Kiggen, B. M. W. Langeveld, A. J. J. M. van Breemen, M. M. de Kok, *Adv. Mater.* **2007**, *19*, 1196.
[157] Y. Jin, S. Nola, K. P. Pipe, M. Shtein, *J. Appl. Phys.* **2013**, *114*, 194303.
[158] N. E. Coates, S. K. Yee, B. McCulloch, K. C. See, A. Majumdar, R. A. Segalman, J. J. Urban, *Adv. Mater.* **2013**, *25*, 1629.
[159] Y. Du, K. F. Cai, S. Chen, P. Cizek, T. Lin, *ACS Appl. Mater. Interfaces* **2014**, *6*, 5735.
[160] Y. Yang, X.-J. Wei, J. Liu, *J. Phys. D: Appl. Phys.* **2007**, *40*, 5790.
[161] S. Ozeri, D. Shmilovitz, *Ultrasonics* **2010**, *50*, 556.
[162] W. B. Phillips, B. C. Towe, P. J. Larson, in *Proc. of the 25th Annual Int. Conf. of the IEEE Engineering in Medicine and Biology Society*, Vol. *25*, IEEE, Cancun, Mexico **2003**, p. 1983.
[163] S. Banerji, W. L. Goh, J. H. Cheong, M. Je, in *2013 IEEE MTT-S Int. Microwave Workshop Series on RF and Wireless Technologies for Biomedical and Healthcare Applications*, IEEE, **2013**, p. 47.
[164] D. B. Christensen, S. Roundy, *J. Intell. Mater. Syst. Struct.* **2016**, *27*, 1092.
[165] Q. Shi, T. Wang, C. Lee, *Sci. Rep.* **2016**, *6*, 24946.
[166] L. Jiang, Y. Yang, R. Chen, G. Lu, R. Li, D. Li, M. S. Humayun, K. K. Shung, J. Zhu, Y. Chen, Q. Zhou, *Nano Energy* **2019**, *56*, 216.
[167] P. J. Larson, B. C. Towe, in *2011 5th International IEEE/EMBS Conf. on Neural Engineering*, IEEE, Cancun, Mexico **2011**, p. 265.
[168] J. Bernstein, K. Houston, L. Niles, K. Li, H. Chen, L. E. Cross, K. Udayakumar, *Integr. Ferroelectr.* **1997**, *15*, 289.
[169] D. Seo, R. M. Neely, K. Shen, U. Singhal, E. Alon, J. M. Rabaey, J. M. Carmena, M. M. Maharbiz, *Neuron* **2016**, *91*, 529.
[170] T. Maleki, N. Cao, S. H. Song, C. Kao, S.-C. A. Ko, B. Ziaie, *IEEE Trans. Biomed. Eng.* **2011**, *58*, 3104.
[171] G. Shin, A. M. Gomez, R. Al-Hasani, Y. R. Jeong, J. Kim, Z. Xie, A. Banks, S. M. Lee, S. Y. Han, C. J. Yoo, J.-L. Lee, S. H. Lee, J. Kurniawan, J. Tureb, Z. Guo, J. Yoon, S.-I. Park, S. Y. Bang, Y. Nam, M. C. Walicki, V. K. Samineni, A. D. Mickle, K. Lee, S. Y. Heo, J. G. McCall, T. Pan, L. Wang, X. Feng, T.-i. Kim, J. K. Kim, Y. Li, Y. Huang, R. W. Gereau, J. S. Ha, M. R. Bruchas IV, J. A. Rogers, *Neuron* **2017**, *93*, 509.
[172] F. Zhang, X. Liu, S. A. Hackworth, R. J. Sclabassi, M. Sun, in *2009 IEEE/NIH Life Science Systems and Applications Workshop*, IEEE, Bethesda, MD, USA **2009**, p. 84.
[173] H. Cao, S. Rao, S.-j. Tang, H. F. Tibbals, S. Spechler, J.-C. Chiao, *Gastrointest. Endosc.* **2013**, *77*, 649.
[174] H. Cao, V. Landge, U. Tata, Y.-S. Seo, S. Rao, S.-J. Tang, H. F. Tibbals, S. Spechler, J.-C. Chiao, *IEEE Trans. Biomed. Eng.* **2012**, *59*, 3131.
[175] T. H. Nishimura, T. Eguchi, K. Hirachi, Y. Maejima, K. Kuwana, M. Saito, in *PESC'94 Record: 25th Annual IEEE Power Electronics Specialists Conference*, IEEE, Taipei, Taiwan **1994**, p. 1323.
[176] S. Y. R. Hui, W. Zhong, C. K. Lee, *IEEE Trans. Power Electron.* **2014**, *29*, 4500.
[177] X. Huang, Y. Liu, H. Cheng, W.-J. Shin, J. A. Fan, Z. Liu, C.-J. Lu, G.-W. Kong, K. Chen, D. Patnaik, S.-H. Lee, S. Hage-Ali, Y. Huang, J. A. Rogers, *Adv. Funct. Mater.* **2014**, *24*, 3846.
[178] G. A. Covic, J. T. Boys, *Proc. IEEE* **2013**, *101*, 1276.
[179] R. A. Bercich, D. R. Duffy, P. P. Irazoqui, *IEEE Trans. Biomed. Eng.* **2013**, *60*, 2107.
[180] E. Y. Chow, A. L. Chlebowski, P. P. Irazoqui, *IEEE Trans. Biomed. Circuits Syst.* **2010**, *4*, 340.
[181] D. R. Agrawal, Y. Tanabe, D. Weng, A. Ma, S. Hsu, S.-Y. Liao, Z. Zhen, Z.-Y. Zhu, C. Sun, Z. Dong, F. Yang, H. F. Tse, A. S. Y. Poon, J. S. Ho, *Nat. Biomed. Eng.* **2017**, *1*, 0043.
[182] S. I. Park, G. Shin, J. G. McCall, R. Al-Hasani, A. Norris, L. Xia, D. S. Brenner, K. N. Noh, S. Y. Bang, D. L. Bhatti, K.-I. Jang, S.-K. Kang, A. D. Mickle, G. Dussor, T. J. Price, R. W. Gereau, M. R. Bruchas IV, J. A. Rogers, *Proc. Natl. Acad. Sci. USA* **2016**, *113*, E8169.
[183] S.-W. Hwang, X. Huang, J.-H. Seo, J.-K. Song, S. Kim, S. Hage-Ali, H.-J. Chung, H. Tao, F. G. Omenetto, Z. Ma, J. A. Rogers, *Adv. Mater.* **2013**, *25*, 3526.
[184] C. H. Lee, H. Kim, D. V. Harburg, G. Park, Y. Ma, T. Pan, J. S. Kim, N. Y. Lee, B. H. Kim, K.-I. Jang, S.-K. Kang, Y. Huang, J. Kim, K.-M. Lee, C. Leal, J. A. Rogers, *NPG Asia Mater.* **2015**, *7*, e227.
[185] H. Tao, S.-W. Hwang, B. Marelli, B. An, J. E. Moreau, M. Yang, M. A. Brenckle, S. Kim, D. L. Kaplan, J. A. Rogers, F. G. Omenetto, *Proc. Natl. Acad. Sci. USA* **2014**, *111*, 17385.
[186] K. Yoshikawa, H. Kawasaki, W. Yoshida, T. Irie, K. Konishi, K. Nakano, T. Uto, D. Adachi, M. Kanematsu, H. Uzu, K. Yamamoto, *Nat. Energy* **2017**, *2*, 17032.
[187] A. N. Bashkatov, E. A. Genina, V. I. Kochubey, V. V. Tuchin, *J. Phys. D: Appl. Phys.* **2005**, *38*, 2543.
[188] E. Moon, D. Blaauw, J. D. Phillips, *IEEE Trans. Electron Devices* **2017**, *64*, 2432.

[189] J. Zhao, A. Wang, M. A. Green, F. Ferrazza, *Appl. Phys. Lett.* **1998**, *73*, 1991.
[190] K. Murakawa, M. Kobayashi, O. Nakamura, S. Kawata, *IEEE Eng. Med. Biol. Mag.* **1999**, *18*, 70.
[191] H. Lorach, G. Goetz, Y. Mandel, X. Lei, T. I. Kamins, K. Mathieson, P. Huie, R. Dalal, J. S. Harris, D. Palanker, *Vis. Res.* **2015**, *111*, 142.
[192] T. Tokuda, T. Ishizu, W. Nattakarn, M. Haruta, T. Noda, K. Sasagawa, M. Sawan, J. Ohta, *AIP Adv.* **2018**, *8*, 045018.
[193] A. Haeberlin, A. Zurbuchen, S. Walpen, J. Schaerer, T. Niederhauser, C. Huber, H. Tanner, H. Servatius, J. Seiler, H. Haeberlin, J. Fuhrer, R. Vogel, *Heart Rhythm* **2015**, *12*, 1317.
[194] K. Song, J. H. Han, T. Lim, N. Kim, S. Shin, J. Kim, H. Choo, S. Jeong, Y.-C. Kim, Z. L. Wang, J. Lee, *Adv. Healthcare Mater.* **2016**, *5*, 1572.
[195] L. Lu, Z. Yang, K. Meacham, C. Cvetkovic, E. A. Corbin, A. Vázquez-Guardado, M. Xue, L. Yin, J. Boroumand, G. Pakeltis, T. Sang, K. J. Yu, D. Chanda, R. Bashir, R. W. Gereau, X. Sheng, J. A. Rogers, *Adv. Energy Mater.* **2018**, *8*, 1703035.